Norwegian University of Life Sciences

Master's thesis 2021 60 ECTS

Faculty of Biosciences (BIOVIT-IPV)
May Bente Brurberg

Functional analyses of *Fvmyb46*-CRISPR/Cas9-edited *Fragaria vesca* plants

Oskar Schnedler Bjorå
Plant science – plant molecular biology

Functional analyses of *Fvmyb46*-CRISPR/Cas9-edited *Fragaria vesca* plants

Oskar Schnedler Bjorå

oskar.schnedler.bjora@nmbu.no

Supervisors

May Bente Brurberg

may.brurberg@nibio.no

Tage Thorstensen

tage.thorstensen@nibio.no

Faculty of Biosciences (BIOVIT) – Department of Plant Sciences (IPV)

Norwegian University of Life Sciences (NMBU)

2021

Acknowledgements

Writing a masters thesis takes hard work and extensive time, and would be impossible for me without the support of various people. I wish to express my sincerest gratitude to the research groups and colleagues I have been involved with at NIBIO.

I would like to thank my supervisors May Bente Brurberg and Tage Thorstensen, whose insight and knowledge in my many queries and discussions helped steer me through my work in this research project. I am forever grateful for your help, both with subject matters and personal motivation during hectic periods.

A very warm thank you goes out to the helpful people at NIBIO: Abdelhameed Elameen, Arti Rai, Monica Skogen, Magne Skårn, Nina Elisabeth Nagy and Vinh Hong Le (and many more!). All our discussions and your help in the laboratory were integral for me to be able to produce this thesis.

Finally, my biggest thanks to my friends and family (including Lila the dog and Cleo the cat) for all the support during my five years of studies at NMBU. I could not have done this without you!

Oskar Schnedler Bjorå

June 2021

Ås, Norway

Abstract

One of the biggest humanitarian challenges in the world today is food security. Improving food production requires improvement in the productivity of existing crops. Plant diseases are major causators of crop yield losses, and generating resistant crops are central to mitigating yields and economical losses by farmers. The application of targeted and precise CRISPR/Cas9 genome editing technology has been a major breakthrough in biological sciences, and can prove to be an important tool for improvement of crop productivity.

The cultivated strawberry (*Fragaria* X *ananassa*) is one of the most important fruit crops in the world, and is susceptible to a wide variety of pathogens. The fungal pathogen *Botrytis cinerea*, which leads to grey mould on a number of species, causes great economical losses on strawberry production worldwide. The wild strawberry (*Fragaria vesca*) is a diploid relative of the cultivated strawberry, and can be regarded as a model species for genetical studies of strawberry. In this thesis, I have investigated the phenotypes of CRISPR/Cas9-edited plants of *F. vesca* with a deletion in the transcription factor-coding gene *FvMYB46* which is predicted to be involved in the regulation of secondary cell wall formation and pathogen susceptibility. Detached leaf and flower assays were carried out along with gene expression analyses of several pathogenesis related genes on material infected and non-infected with *B. cinerea*, to see whether the deletion led to higher resistance to the pathogen. No changes in resistance were observed between *myb46* mutants and control plants; however, a few genes related to pathogenesis were less expressed in *B. cinerea* infected *myb46* mutants, suggesting that a deletion in *MYB46* changes the gene expression response upon pathogenic infection.

Wild type and *myb46* mutant plants were then analysed to see differences in secondary wall lignin deposition of floral stems;. Microscopy evidence suggested that lignin deposition in secondary cell walls is downregulated in *myb46* mutants compared to controls, indicating that *MYB46* plays a role in secondary cell wall deposition. Finally, detached leaves were exposed to different levels of osmotic stress to investigate drought tolerance These results indicated that leaves of *myb46* mutants may be more susceptible to drought stress than wild type plants.

From the experiments conducted in this study, it seems that *MYB46* is not involved in resistance to grey mould in *Fragaria*. However, the data in this study suggest that *MYB46* may be involved in regulation of drought stress responses and cell wall composition.

Table of contents

1 Introduction:

1.1 Background

One of the biggest humanitarian challenges in the world today is food security. The United Nations estimate that around 8.9 % of the world population suffers from hunger (UN, 2019a). Furthermore, it is estimated that the world population will reach 10 billion people by 2050 (UN, 2019b), demanding that food production increases along with the increasing population size. Improving food production requires improvement in multiple areas, including agricultural practice, infrastructure and the productivity of existing crops.

Among the biggest biotic causators of crop yield losses are plant diseases. Plant diseases are caused by fungi, bacteria, viruses and even nematodes; of them, one of the most detrimental groups being plant fungal pathogens (*phytopathogens*). They require high fungicide use and cause damaged crops, threatening food security and livelihoods of farmers as well as food safety and pollution. To mitigate the effects of plant diseases, generating resistant varieties and improving agricultural management are important solutions.

The use of fungicides for preventing and mitigating pathogenic outbreaks is common practice in the cultivation of most plant cultures. The practice is, however, a double-edged sword due to it having multiple negative consequences. Excessive and uniform fungicide use can lead to selection for fungicide resistance. Moreover, the chemicals within can pollute, and may have high ubiquity in water and soil. For many crops, postharvest application of fungicides is common, raising health questions on the presence of fungicide residues during consumption.

Generating crops resistant to diseases is a key element in disease management, and has been practiced through breeding for around a century. However, the types of resistance achieved through conventional plant breeding are often overcome due to pathogens selecting for virulent strains (Elisabeth Lof et al., 2017). In recent times, gene editing techniques that are easy-to-implement, cheap and precise such as CRISPR-Cas9, have emerged. The precision of these techniques show potential for allowing researchers to generate more durable resistance.

1.2 Strawberry:

Cultivated strawberry (*Fragaria* X *ananassa* Duch. ('X' from a crossing between older species of *Fragaria*)) is part of the *Rosaceae* family. Its domestication is estimated to have occurred as late as in the 1700s (Edger et al., 2019) and is now regarded among the most important fruit crops in the world (Bestfleisch et al., 2015). Its edible parts are neither berries nor true fruits; the achenes surrounding the fleshy, edible parts originate from the ovaries.

Despite botanically as such being “false fruits”, they are referred to as fruits or berries in this thesis. In addition to generative (sexual) formation by seed-containing fruits, strawberry plants form vegetatively (asexually) by generating stolons. Plants formed from stolons are clones of the mother-plant. Different strawberry cultivars are abundant, and strawberries are highly affected by their climatic conditions; this together makes *F.* X *ananassa* a highly variable species (Garrido et al., 2011). Strawberry fruits are non-climacteric, meaning that they do not ripen after harvest.

Strawberry is susceptible to a large variety of phytopathogens (Amil-Ruiz et al., 2011).The most important group of pathogens affecting strawberries are fungi; it is in fact affected by more than 50 genera of pathogenic fungi (Williamson et al., 2007). Different cultivars differ widely in terms of resistance against certain pathogens. Additionally, cultivars in different climates and regions may differ in resistance; a cultivar in one region may be susceptible to a certain pathogen, and in another region not, because of the climatic conditions as well as the different strains present. There is to this date an absence of strawberry cultivars exhibiting high resistance to multiple pathogens (Nellist, 2018).

According to FAOSTAT, annually more than 8 million tons of strawberries are produced worldwide, on an area of around 370.000 hectares (FAOSTAT, 2020). In Norway, in 2019 around 9.000 tons of strawberries were produced on an area of around 1.300 hectares (SSB, 2020). The amount of farms producing strawberries in Norway have declined over the last 40 years, despite the total production area being relatively stable (SSB, 2018), suggesting that mainly large-scale farmers contribute to strawberry production. Moreover, Norwegian strawberry import has increased greatly over the years (SSB, 2018), implying that the demand is far greater than farmers are able to produce.

The genome of *F.* X *ananassa* is allooctoploid (2n = 8x = 56), with an estimated genome size of 813.4 mb (mega base pairs). High ploidy, a large genome and a generally high level of heterozygosity has made assembly and mapping of its genome challenging (Edger et al., 2019). Moreover, cultivated strawberry is intolerant to inbreeding. This, coupled together with a complex genomic composition makes breeding for new strawberry cultivars lengthy and difficult (Wilson et al., 2019).

The wild strawberry (*Fragaria vesca*) is a closely related species of the cultivated strawberry. Its genome is diploid and is considerably smaller (240 mb) than its cultivated relative. (Shulaev et al., 2011) reported the whole-genome sequence of *F. vesca ssp. vesca* Hawaii 4

(known as H4x4) (National Germplasm Repository accession #PI551572), an ecotype self-fertilized four times. This ecotype produces white/yellow fruits and can complete its life cycle in 4 months. *F. vesca* H4x4 can be regarded as a model plant for the *Fragaria* genus, and likely for other related *Rosaceae* plants (Shulaev et al., 2011), such as apples and roses.

1.3 Grey mould

The causal pathogen of grey mould, *Botrytis cinerea*, is a fungal necrotrophic pathogen belonging to the phylum ascomyceta. It is the causative agent of grey mould on a wide range of horticulturally cultivated plants, causing soft rot on all above-ground plant parts (Williamson et al., 2007). Diseases of *Botrytis*, caused mainly by *B. cinerea* and a few other species, are the most common diseases of greenhouse-grown crops (Agrios, 2005). Annual global economic losses from *B. cinerea* vary between 10 billion and 100 billion USD (Watkinson et al., 2016), with a great portion affecting strawberry production. Economical losses from *B. cinerea* are caused not only by yield losses, but also by preventative anti-fungal measures such as fungicide application and less time-effective handling practices.

1.3.1 Infection

Since *B. cinerea* is mainly a necrotrophic pathogen, it takes advantage of weakened and dead plant material. It is as such considered a weak parasite (Williamson et al., 2007); however, it is able to locally infect healthy plant tissue in a short, biotrophic phase up until senescence or ripening (Petrasch et al., 2019), and can actively kill host cells in order to establish infection (AbuQamar et al., 2017). Relatively young as well as old plant tissue usually is more susceptible to infection from *B. cinerea*. In *F.* X *ananassa*, susceptibility to *B. cinerea* decreases dramatically from 1 – to 4-week-old leaves, and subsequently increases as leaves turn 5 weeks or older (Meng et al., 2019).

1.3.2 Symptoms:

Leaves, stems, seeds, inflorescences and fruits of strawberries can be infected by grey mould. Although it can cause disease on all above-ground plant parts, disease pressure is most present during flowering (Bristow et al., 1986). Leaves and stems that are infected will start to wilt, turning brown and soft; eventually, fungal growth as mycelial clusters on the leaves may appear. On inflorescences, infection is established quite rapidly, producing abundant mycelium typically after fruit emergence (Agrios, 2005). Infection often begins in the inflorescences, where the fungus grows and spreads to the petals, further spreading to the fruit where it causes blossom end rot symptoms. Infected fruits become brown and soft, and sclerotia can appear on infected fruits over time.

1.3.3 Life cycle:

B. cinerea is a polycyclic pathogen. It produces gray mycelium and long, branched conidiophores in abundance, resembling clusters of grapes when seen through a microscope. In the winter, the fungus overwinters in soil as mycelium on decaying plant material, or as sclerotia. However, the pathogen is active at temperatures above 0° C. Upon germination of sclerotia, clusters of grape-like conidiophores bearing conidia spread, infecting the host. Conidia are primarily spread by wind currents, but can also be dispersed by water droplets. For sporulation, infection, germination and growth, humid conditions and temperatures between 18 and 26 °C are required (Agrios, 2005).

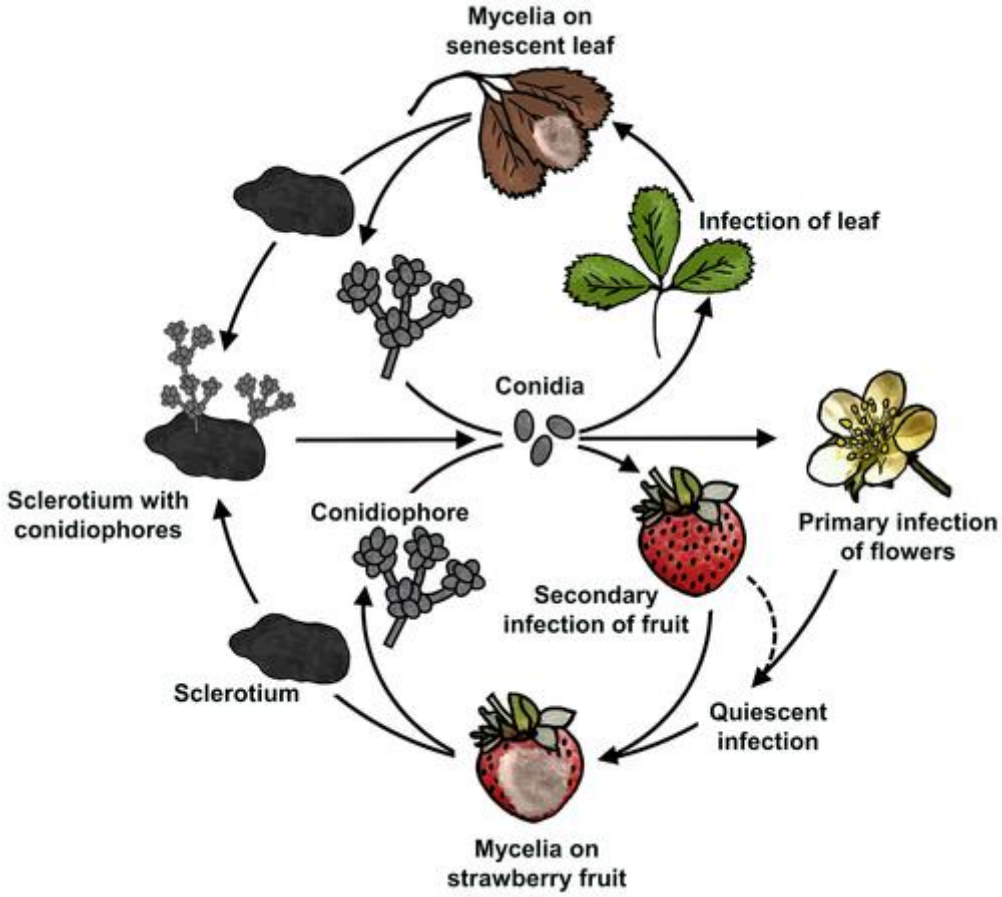

Fig 1.3.1: *Illustrated disease cycle of B. cinerea and its infection on strawberries. The pathogen overwinters primarily in sclerotia, but also as mycelium in soil or plant debris. Primary infection occurs mainly on flowers, and becomes visible during and after fruit development. Figure obtained from (Petrasch et al., 2019).*

1.3.4 Disease control:

Due to the potential economic impact of disease outbreaks in strawberry fields, proper disease control is imperative. Removal of infested plant material and maintaining low air humidity in greenhouses are simple preventative measures taken by strawberry producers.

Normal measures in control of *Botrytis* are the use of fungicides (*botryticides*), both curatively and preventatively. Ultimately, a mix of chemical and cultural methods is required for control of grey mould. Application of botryticides and broad spectrum fungicides during strawberry flowering is common practice, and in some cases, post-harvest fungicides are applied to ensure sufficient strawberry shelf life (Huang et al., 2011). On the other hand, fungicides are often expensive and inconsistently effective (Petrasch et al., 2019). Additionally, some fungicides persist long in water and soil and are toxic to many living organisms. Sustained use of fungicides can, and often will, lead to selection of fungicide resistant strains; (Bestfleisch et al., 2015) report several cases of botryticide resistant strains. It is of great importance that we find alternative ways of disease control, to reduce the unsustainable effects of long-term fungicide use.

Producing resistant cultivars is a central strategy in disease mitigation. Strawberry cultivars that are completely resistant to *B. cinerea* do not exist. Degrees of partial resistance has been found in some cultivars, but they often come with concomitantly less desirable traits (Bestfleisch et al., 2015). Finding resistant cultivars still remains a challenge, but the lack of success could be a result of the wrong approaches in resistance breeding. There are no standardized tests for resistance, and cultivar testing often focuses on traits such as yield and ripening time rather than resistance against pathogens. Coming up with standardized tests for resistance would allow for more goal-oriented breeding, meanwhile allowing for better sharing and comparing of results across the plant scientific community (Bestfleisch et al., 2015).

1.4 Gene editing technology:

Ever since the first Agricultural Revolution around 10.000 years ago, humans have practiced plant breeding through selection of plants with desirable traits, albeit unintentional up until around the 1900s. Intentional plant breeding intensified within the last 100 years, and has been the most successful approach in the development of new plant species (Borrelli et al., 2018). In the later decades of the 20th century, genetic modification and gene editing were made possible. Genetic modification traditionally involves the introduction of a foreign gene from one organism to another, and has been used commercially for a few decades, with the first commercial biotech-crop emerging in 1996 (Maghari & Ardekani, 2011). Gene editing normally introduces no foreign genes, instead deleting and thus altering the genomic base pair arrangements; this makes gene editing an approach that seems to be of wider public accept than the more traditional genetic modification (Kato-Nitta et al., 2019). With the emergence

and improvement of gene editing technologies, scientists are now able to actively edit the genome of plants as well as other organisms, accurately altering desired traits such as disease resistance without necessarily having to introduce a foreign gene. The potential for gene editing technology shows promise, however it remains to see to which degree its potential will be achieved.

Genome editing of plants is a process requiring thorough design and planning. Gene editing for pathogenic resistance often demands knowledge about the pathogen's infection mechanisms as well as the plant's defense mechanisms. Knowing which types of mutations are desired or even whether to target the host or the pathogen are all elements that must be assessed. Additionally, designing a method for the gene engineering itself is an important and tedious process.

In the 2010s, Emmanuelle Charpentier and Jennifer A. Doudna developed a method for gene editing called CRISPR/Cas9 (Clustered Regularly Interspaced Short Palindromic Repeats/CRISPR-associated protein 9). The discovery and implementation of CRISPR/Cas9, which in 2020 earned Charpentier and Doudna the Nobel Prize in chemistry, has been a revolutionary breakthrough within biological sciences. CRISPR/Cas9 is easy and cheap to implement and has a high success rate, even for multiplex genome editing (Borrelli et al., 2018); making it a highly preferred technique for gene editing experiments.

In essence, CRISPR/Cas9 is utilized to cut and, in some cases, replace specific genomic sequences. CRISPR/Cas9 originates from the bacterium *Streptococcus pyogenes*, wherein the system's role is to acquire and maintain immunity to foreign viruses. Cas9 is an endonuclease that adaptively recognizes and cuts PAMs (Protospacer Adjacent Motifs), short sequences found in the viral genomes that are foreign to the *S. pyogenes* genome. It then inserts part of the cut sequence into its own genome, to serve as a memory for future infections by the same virus. In practice, scientists are able to make use of the adaptive CRISPR/Cas9 systems and engineer them to make targeted gene edits. (Borrelli et al., 2018)

Cas9 is guided by a single guide-RNA (sgRNA), consisting of CRISPR RNA (crRNA) and trans-activating RNA (tracrRNA). The sgRNA guides Cas9 by binding close to the PAM site, where the Cas9 complex cleaves the DNA adjacent to the PAM sequence (Borrelli et al., 2018). After the Cas9 nuclease has cleaved the targeted DNA, a double-strand break is generated. These breaks are repaired by non-homologous end joining (NHEJ) or homology-directed repair. NHEJ is an error-prone process, as it simply rejoins the broken ends,

regardless of the homology of the strands. This can cause insertion or deletion mutations, which might be favorable when knock-out mutants are desired. Homology-directed repair often makes error-free repairs, and can be best utilized in gene replacement and knock-in editing of plants (Song et al., 2016).

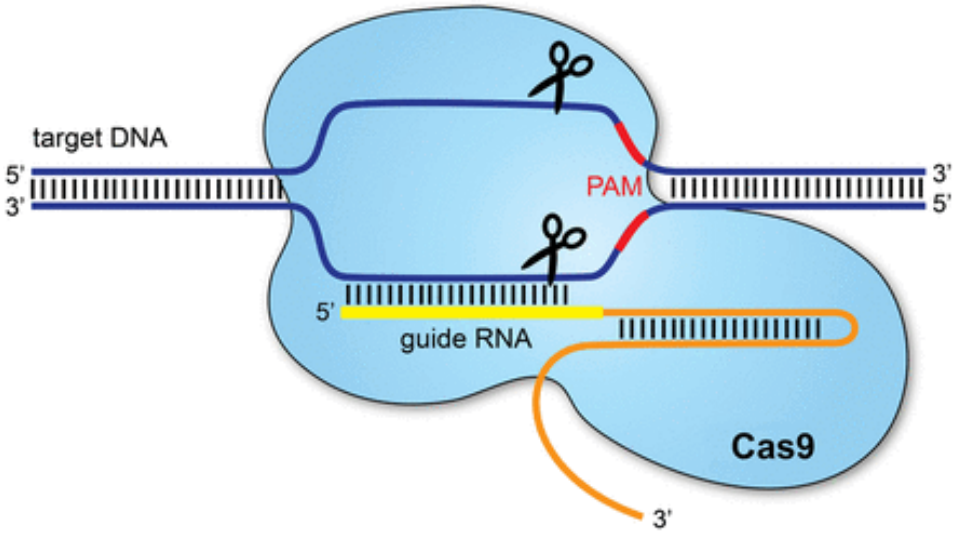

Fig 1.5.1: *A simple illustration of the activity of CRISPR/Cas9. After expression of Cas9, it is guided to the target site by a sgRNA of 18-20 bp length. In order to cut, a specific PAM sequence at the 3' end directly following the target genomic section corresponding to the sgRNA must be present. Illustration obtained from (Redman et al., 2016).*

Expression of Cas9 in an organism needs to be enhanced by help of specific promotors. In plants, the *Cauliflower mosaic virus* 35S is commonly used (Belhaj et al., 2013). In addition to using specific promoters for expression of Cas9 in the nuclei, specific sequences for the sgRNAs are modified, to confer target specificity. The guide sequence of the sgRNA consists of 18-20 bp (base pairs) that target the genomic DNA. The expression of the sgRNAs is controlled by plant RNA polymerase III promoters, such as U6 and U3 (Belhaj et al., 2013).

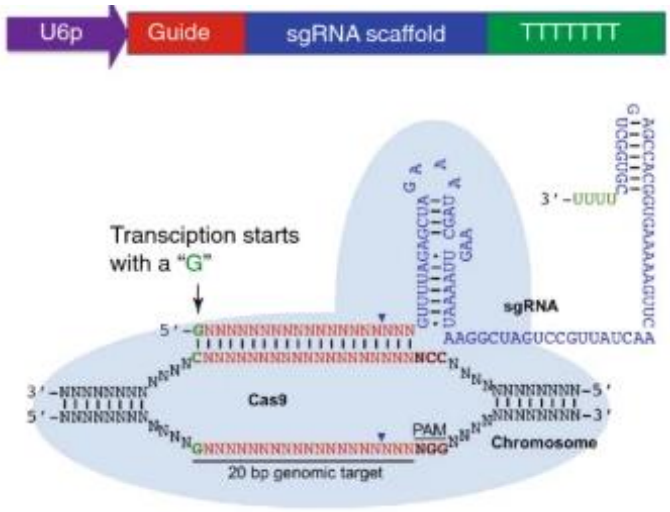

Fig 1.5.2: *An example of Cas9 activity in plants. Cas9 is guided to the cut site by the sgRNA, of which expression is driven by a promotor (in this case U6p, by which transcription is initiated by a "G"). Illustration obtained from. (Belhaj et al., 2013)*

The use of CRISPR/Cas9 is already applied in a variety of organisms, including plants. In plants, specific Cas9-like enzymes that are optimized to plant codons have been used, of which the most widely explored is Cpf1, now called Cas12, from *Prevotella* and *Francisella* (Borrelli et al., 2018)(In this thesis, Cas9 was used). The use of CRISPR/Cas9 in developing plants resistant to diseases has shown promise. Several success stories exist in developing plant resistance to pathogens using CRISPR/Cas9, such as conferring resistance to Begomoviruses (Borrelli et al., 2018), enhancing defense responses in cocoa (*Theobroma cacao*) (Fister et al., 2018) and reducing disease severity of Cassava brown streak disease in cassava (*Manihot esculenta*)(Gomez et al., 2019). While other recently developed gene editing techniques exist, such as zinc-finger nucleases and transcription activator-like effector nucleases, CRISPR/Cas9 seems to be the predominant gene editing technique used. CRISPR/Cas9 has proven to be a key discovery in not only plant pathology, but in most biological sciences (Borrelli et al., 2018).

1.5 Plant defense:

Plants have evolved diverse strategies to combat attacks from microbial agents. Once a pathogen is detected, signaling networks are activated by generating small molecules and balancing hormonal signaling pathways, initiating defense mechanisms (AbuQamar et al., 2017). Unlike vertebrates, plants lack an adaptive immune system and mobile immune cells (Han, 2019). Plants mainly rely on the innate (or *basal*) immune system of each cell as well as systemic signals of infection to respond to microbial interactions (Jones & Dangl, 2006).

Essentially, there are two branches of the plant immune system. One branch uses pattern recognition receptors (PRRs) located on the cell surface to detect microbial -or damage associated molecular patterns (MAMPs or DAMPs, respectively). The other branch utilizes resistance by endocellular expression of nucleotide binding-leucine rich repeat (NB-LRR) proteins encoded by resistance genes (R-genes) to respond to effector molecules (or *virulence factors*) secreted by the pathogen (Han, 2019).

Both branches of the plant basal immune system are involved in different stages of pathogenic immune responses. Extramembranous recognition of PAMPs by PRRs activates pattern triggered immunity (PTI). Examples of PRRs are receptor-like kinases- and proteins (RLKs and RLPs). DAMPs are signals elicited by the plants itself upon stress, and are also extramembranously recognized, activating a PTI. Pathogens can, however, inhibit PTI responses intracellularly by secretion of effector molecules; this is referred to as effector-triggered susceptibility (ETS). These effectors can in turn be recognized by NB-LRR proteins, which activates an effector-triggered immunity (ETI) response. ETI is a strong defense response, and in many cases leads to a hypersensitive response (HR) (Jones & Dangl, 2006) (Balint-Kurti, 2019). HRs cause localized cell death at the recognized pathogenic infection site.

In nature, resistance against pathogens is often overcome due to the pathogen having to overcome single molecular patterns (van Schie & Takken, 2014). To illustrate the phases of susceptibility and immunity in host-pathogen interactions, a zigzag model is often used. It is a good model for explaining susceptibility and resistance as an evolutionary arms-race between hosts and pathogens. However, it is best used for illustrating host-pathogen interactions when the pathogen is biotrophic or hemi-biotrophic (Keller et al., 2016), and is not as applicable for necrotrophic pathogens.

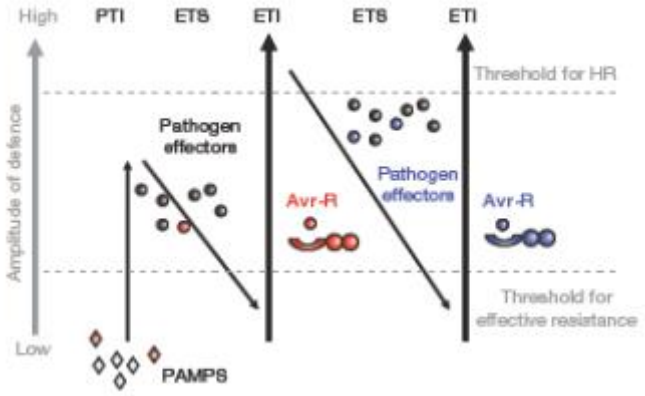

Fig 1.4.1: *The zigzag model for resistance. The amplitude of defense is proportionate with [PTI-ETS+ETI]. Recognition of PAMPs lead to PTI. Pathogen effectors can in turn override PTI, leading to susceptibility (ETS). If proteins encoded by R-genes recognize these effectors, ETI is attained, typically leading to a HR. Over generations, selection leads to pathogens evolving effectors that are no longer recognized by any NB-LRR proteins; this anew renders the host susceptible until the host itself eventually has selected for R-genes. Illustration from (Jones & Dangl, 2006).*

As well as resistance genes, susceptibility genes persist in nature. Defense mechanisms involve the expression of resistance genes upon infection, or the lack of expression of susceptibility genes. By targeting susceptibility genes in plant breeding and gene editing, more durable and broad resistance could be achieved (van Schie & Takken, 2014). Susceptibility genes may primarily serve a beneficial role to the host, but render the plant susceptible to pathogenic infection through pleiotropic effects. Consequently, inhibiting the function of a susceptibility gene may lead to an overall loss of fitness. A classic example of susceptibility genes is *MLO* (Mildew Locus O), which confers susceptibility to powdery mildew in a wide range of cultivated plants (Kusch & Panstruga, 2017). The resistance to powdery mildew is attained when *MLO* is non-functional, hence when it is recessively or not at all expressed. In studies by (Babaeizad et al., 2009) and (Eichmann et al., 2010), the barley (*Hordeum vulgaris*) susceptibility protein BAX-INHIBITOR-1 (BI-1), which is partially regulated by *MLO*, was shown to confer susceptibility to powdery mildew. When expression of *BI-1* was reduced, a trade-off was observed, rendering barley more susceptible to necrotrophic pathogens. (Hückelhoven et al., 2013)

1.5.1 Defense against grey mould

Grey mould (*B. cinerea*) is, as earlier mentioned, a broad-host-ranged, nectrotrophic pathogen. It primarily takes advantage of weakened and dead tissue, such as necrotic lesions caused by HRs; however a biotrophic phase of *B. cinerea* has been observed (Petrasch et al., 2019) and the pathogen itself is able to kill host cells. Although *B. cinerea* is a ubiquitous pathogen that is yet to be effectively mitigated, various defense strategies have been observed in plants.

Both MAMPs and DAMPs are involved in plant resistance against *B. cinerea*. Upon infection, the fungal cell wall constituent chitin is recognized as a MAMP by certain extramembranous RLKs. As observed in plants of mouse-ear cress (*Arabidopsis thaliana)*, DAMPs are released by the plant cell wall in the form of oligogalacturonides (OGs) upon damage by *B. cinerea*. OGs are detected by Wall-Associated Kinase 1 (WAK1), consecutively activating defense

responses. Overexpression of WAK1 confers increased resistance to *B. cinerea* (Brutus et al., 2010). Polygalacturonase-inhibiting proteins (PGIPs), which inhibit the effector-like function of polygalacturonases, have been shown to increase resistance to *B. cinerea* when overexpressed (De Lorenzo et al., 2011). (AbuQamar et al., 2017)

Maintaining and optimalizing hormonal signalling in plants is important for combating pathogens. The phytohormones salicylic acid (SA), jasmonic acid (JA), ethylene (ET), abscisic acid (ABA) and brassinosteroids (BR) are known to play a central role in defense against *B. cinerea* (AbuQamar et al., 2017). Salicylic acid has been shown to induce expression of *PR1*, and subsequently resistance against *B. cinerea* in *A. thaliana* (Ferrari et al., 2003). Phytohormones are individually, but also interconnectedly, contributors to plant defense against *B. cinerea*. (AbuQamar et al., 2017)

1.5.2 The cell wall

Cell walls of plant cells serve a multitude of functions. They not only help maintain structural support and rigidity, but also help prevent infection by pathogens or pests (Evert & Eichhorn, 2013). After cellular expansion, plant cells that need structural reinforcement may develop a secondary cell wall (Miedes et al., 2014). Secondary cell walls are mainly composed of cellulose, hemicellulose and lignin. Lignin is thought to have emerged primarily as a ways for plants to prevent infections by pathogens, and later gained the function of waterproofing and supporting xylem tissue, thus providing rigidity (Evert & Eichhorn, 2013). Studying the function of, and involvement of lignin in defense against pathogens can be important for developing plant resistance.

1.5.3 Strawberry defense

Strawberry is prone to disease from a wide range of pathogens. Natural resistance to pathogens has been observed in strawberry, however it seems that it is often polygenic and quantitatively inherited (Amil-Ruiz et al., 2011). Strawberry fruits are prone to physical damage which frequently leads to breaking down of the mechanical barrier towards pathogenic infection. Direct links between fruit firmness and susceptibility have been observed (Gooding, 1976). It is expected that studying genes involved in modification of the cell-wall will be useful for understanding the processes of resistance against pathogens in strawberry (Amil-Ruiz et al., 2011).

1.6 *MYB46*:

MYB46 (*MYB proto-oncogene 46*) is a gene coding for the MYB transcription factor MYB46 in *A. thaliana*. MYB transcription factors in plants control processes such as differentiation,

development and abiotic processes (Guo et al., 2017), and are present in all eukaryotic organisms (Ambawat et al., 2013). MYB46 acts redundantly with another MYB protein, MYB83, in regulating cell wall biosynthesis in *A. thaliana* (McCarthy et al., 2009). Expression of *MYB46* is targeted directly by *SND1*, a gene coding for SECONDARY WALL-ASSOCIATED NAC DOMAIN PROTEIN1 (SND1), a major transcriptional activator in cell wall synthesis (Zhong et al., 2007). MYB46 targets another MYB gene, *MYB85*, and *KNAT7* (*KNOTTED-LIKE HOMEOBOX OF ARABIDOPSIS THALIANA 7*), both genes involved in secondary wall synthesis in inflorescences in *A. thaliana*. Furthermore, it targets the cellulose synthase genes *CESA4*, *CESA7* and *CESA8*, which also are involved in secondary wall formation (Ramirez et al., 2011b).

(Ramirez et al., 2011a) found that plants of *A. thaliana* with a deletion in the *MYB46* gene had higher leaf resistance to grey mould (*B. cinerea*). Moreover, they found that there were changes in lignin deposition in inflorescence xylem secondary walls, varying with sequential genomic deletions (Ramirez et al., 2011a). *MYB46* is thus affected differently depending on the specific affected sequence.

Alteration of *MYB46* may control various phenotypic changes across plant species. (Guo et al., 2017) discovered that overexpression of the birch (*Betula platyphylla*) *MYB46* resulted in increased osmotic stress tolerance. Additionally, this overexpression led to increased lignin and cellulose content, and reduced hemicellulose content. In another study by Cheng and colleagues (Chen et al., 2019), similar findings were done in apple (*Malus domestica*); overexpression of *MYB46* led to increased salt- and osmotic stress tolerance, as well as changes in lignin content. There are potentially a number of functions affecting phenotypic traits by *MYB46* in different plant species.

Before my involvement in this project at NIBIO, *F. vesca* plants were genetically edited by CRISPR/Cas9 and maintained in greenhouse. A spCAS9-TPC vector, containing Cas9 optimized for plants was used for a targeted ≈81-base pair deletion of the *Fragaria vesca MYB46* (*FvMYB46*) gene, a putative homolog of *A. thaliana MYB46* (*AtMYB46*) (Tage Thorstensen, unpublished).

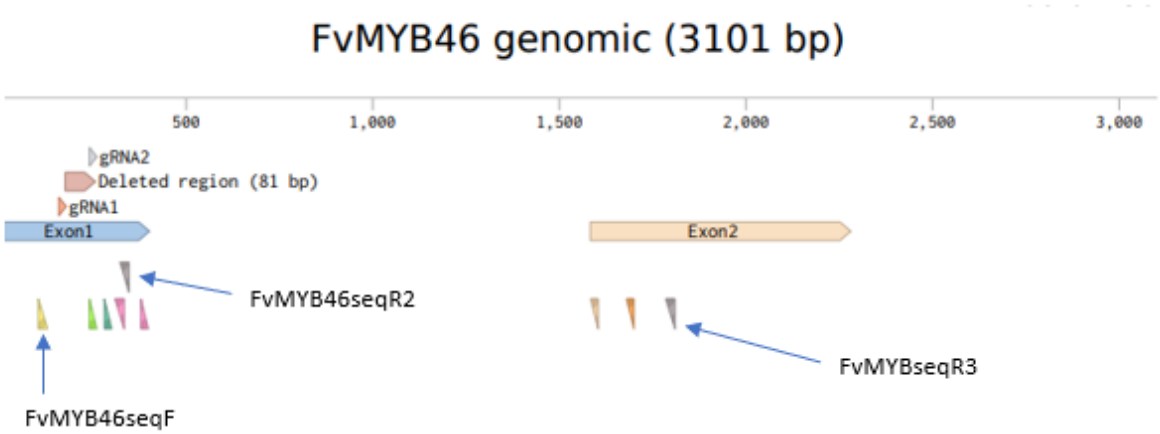

Fig 1.7.1: *Illustration of the FvMYB46 genomic sequence and the deletion generated, along with the primers FVMYB46seqF, FVMYB46seqR2 and FVMYB46seqR3, which flank the deleted sequence. Illustration obtained from Benchling.*

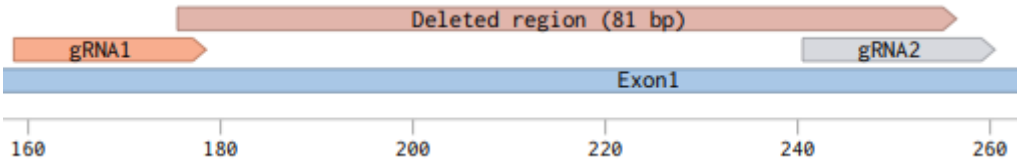

Fig 1.7.2: *A closer look at the 81-bp deletion in FvMYB46 and the gRNAs for insertion. The deleted region is within the same exon. Illustration obtained from Benchling.*

In this thesis, I worked further with the CRISPR-Cas9 edited plants of *Fragaria vesca*, to investigate resistance against *B. cinerea*, lignin differences as well as osmotic stress tolerance.

The main hypothesis of the study is that *FvMYB46* acts as a susceptibility gene to *B. cinerea* as observed in *AtMYB46* (Ramirez et al., 2011a).

Main objectives:

The main objective was to test the hypothesized resistance of *myb46* to *B.* cinerea.To study the effects of a deletion in *MYB46* in *F. vesca*, phenotypic tests were performed. Detached leaf assays as well as detached flower assays were carried out. The aim of this was to investigate any difference in *B. cinerea* infection on plants with and without a deletion in *MYB46*. To find out if the absence of *MYB46* affects the plant's defense response upon infection with *B. cinerea*, expression was analysed using qPCR.

Secondary objectives for the thesis:

- Observe phenotypic traits of *Fvmyb46* mutants during growth
- Investigate the segregation of generatively formed descendants of the transgenic lines
- Investigate possible homologous genes from the *AtMYB46* pathway
- Investigate differences in lignin contents of infected and non-infected mutants and wild-type by use of microscopy
- Investigate whether *myb46* plants exhibit different phenotypes when exposed to drought stress than their wild-type counterpart

2 Materials

Table overviews of chemicals, laboratory equipment and softwares used in the experiments are presented in tables 2.1 to 2.8

Table 2.1 Chemicals

Chemical	Supplier
Agarose	Sigma-Aldrich, St. Louis, MO, USA
Boric acid	Sigma-Aldrich, St. Louis, MO, USA
Cetyltrimethylammonium Bromide (CTAB)	Sigma-Aldrich, St. Louis, MO, USA
Chlorine (Klorin)(Sodium hypochlorite) 4 %	Lilleborg, Oslo, Norway
Chloroform:Isoamylalcohol (24:1)	Thermo-Fischer Scientific, Waltham, MA, USA
DNA Gel Loading Dye (6X)	Thermo-Fischer Scientific, Waltham, MA, USA
dNTP nucleotides	Thermo-Fischer Scientific, Waltham, MA, USA
Ethanol 96 %	VWR chemicals, Radnor, PA, USA
Ethidium Bromide	Sigma-Aldrich, St. Louis, MO, USA
Ethylenediaminetetraacetic acid (EDTA)	Sigma-Aldrich, St. Louis, MO, USA
Glutaraldehyde	TAAB Laboratories Equipment, Aldermaston, Berks, England
HCl	Sigma-Aldrich, St. Louis, MO, USA

NaCl	Merck KgaA, Darmstadt, Germany
NaOH	Sigma-Aldrich, St. Louis, MO, USA
Nitrogen (l)	AGA, Norway
Mannitol 98%	Sigma-Aldrich, St. Louis, MO, USA
Para formaldehyde	Sigma-Aldrich, St. Louis, MO, USA
Pipes	Sigma-Aldrich, St. Louis, MO, USA
Polyvinylpolypyrollidone (PVPP)	Sigma-Aldrich, St. Louis, MO, USA
Tris-base	Sigma-Aldrich, St. Louis, MO, USA
Trizma®-hydrochloride (Tris-HCl)	Sigma-Aldrich, St. Louis, MO, USA
Tween ® 20	Sigma-Aldrich, St. Louis, MO, USA
β-mercaptoethanol	Sigma-Aldrich, St. Louis, MO, USA

Table 2.2 Solutions

Solution	Reagent	Volume
1 X TBE buffer	Tris-base	108 g
	Boric acid	55 g
	EDTA (0.5 M)	40 mL
	Distilled H_2O	Up to 1 L
4% Para formaldehyde	Para formaldehyde	4 g/ 100 mL dH_2O
	NaOH	To 1M
CTAB-buffer	CTAB 2 %	2 %
	EDTA	25 mM
	NaCl	1 M
	PVPP	2 %
	Tris-HCl	100 mM
	ß-mercaptoethanol	1 %
Pipes buffer 0.1M	Pipes	34.63 g/ 1 L dH_2O
	HCl	To pH 7
Potato Dextrose Broth	Potato	4 g
	Dextrose	20 g
	Distilled H_2O	To 1 L

Table 2.3 Equipment

Equipment	Model	Supplier
Centrifuge	CVP-2	Grant Instruments Ltd, Cambridgeshire, UK

Centrifuge	Heraeus Pico 21	Thermo-Fischer Scientific, Waltham, MA, USA
Electrophoresis visualizer	Gel Doc™ EQ	Bio-Rad, Hercules, CA, USA
Fluorescence lamp	ebq 100	Leica Microsystems GmbH, Wetzlar, Germany
Heatblock	Thermo-Shaker PSC24	Thermo-Fischer Scientific, Waltham, MA, USA
Incubator	Versatile Environmental Test Chamber MLR-351H	Panasonic, Kadoma, Osaka, Japan
Laminar flow cabinet	Herasafe™ KS, Class II Biological Safety Cabinet, MS12	Thermo-Fischer Scientific, Waltham, MA, USA
Microscope	DM LS40	Leica, Wetzlar, Germany
PCR instrument	T100™ Thermal Cycler	Bio-Rad, Hercules, CA, USA
qPCR instrument	CFX96™ Real-Time System	Bio-Rad, Hercules, CA, USA
Spectrophotometer	Nanodrop™ 2000	Thermo-Fischer Scientific, Waltham, MA, USA

2.4 Kits

Kit	Supplier
DNase I Amplification Grade Kit	Sigma-Aldrich, St. Louis, MO, USA
Dneasy ® Plant Mini Kit	Sigma-Aldrich, St. Louis, MO, USA
iScript™ Advanced cDNA Synthesis Kit for RT-PCR	Bio-Rad, Hercules, CA, USA
Spectrum™ Plant Total RNA Kit	Sigma-Aldrich, St. Louis, MO, USA

2.5 Softwares

Software	Supplier/developer
Benchling	Benchling inc., San Francisco, CA, USA
Bio-Rad CFX Manager	Bio-Rad, Hercules, CA, USA

BLAST (Basic Local Alignment Search Tool)	National Center for Biotechnology Information, U.S National Library of Medicine, Bethesda, MD, USA
Excel	Microsoft, Redmond, WA, USA
ImageJ	National Institutes of Health, Bethesda, MA, USA
Quantity One	Bio-Rad, Hercules, CA, USA

2.6 Primers

Oligo name	Oligo sequence (5'-3')
Cas9 F3n	CAACAACTACCACCACGCTCA
Cas9 R3n	ATCCCTTCCCTTATCCCACAC
Flank_upstream_TDNA2_2_F	AATGGTCAAAATACCACATAGGC
FvBG2-3RTF	CCCTAATAAACAGCCAAAGTATCAGC
FvBG2-3RTR	CAACACTGTTCTTCAATATAGCGAC
FVCSA4 F	GGCGACAAAGAAGCTTTGGG
FVCSA4 R	CCGAGCTTCAGCCATTAGGA
FVCSA4-2 F	GATGGGTGATGCAGGATGGT
FVCSA4-2 R	ACAAGACGTGGCAGTTCCTT
FVCSA7 F	TTCATGGTCACGAAGAGCACA
FVCSA7 R	ACTATAGCAAGGCCTGCAC
FVCSA7-2 F	GGAGATGGTGCAAACCTCCA
FVCSA7-2 R	CTTGAGGAAGGAGGCACACC
FVCSA8 F	AATGAGCTTCCTCGGTTGGT
FVCSA8 R	CAGACACCCTTACCAGGGC
FVCSA8-2 F	TCCCCTATTTGCAGGGCTTG
FVCSA8-2 R	GCTCAGCCAGTGTCTTCTCA
FV_EF1-α-RTF	GCCCATGGTTGTTGAAACTTT
FV_EF1-α-RTR	GGCGCATGTCCCTCACA
FVKNAT7 F	AGTGTTGTGCTCGTTCAAGG
FVKNAT7 R	CACCCAGGGTAACTCCGGTA
FVKNAT7-2 F	GAGCGCCAAGAGCTCGATAA
FVKNAT7-2 R	GCCTGCAAGGTGCTTTCAAT
FVMYB46_F	GAACCCTATGCTGTAAGTAATACCG
FV_MYB46_QPCR_F	GAGAGGTGCGGAAAGAGTTG
FV_MYB46_QPCR_R	CCATTTCCATTCCCTTCTTG
FV_MYB46_QPCR_F2	CTGCAATTTGAGACCACCTG
FV_MYB46_QPCR_R2	CAGTGGAGGAGGAGGAGGAC
FV_MYB46_Rseq2	ACCTCTCTTAAGGTCAGGTCTCAA
FV_MYB46_Rseq3	CATCATTGACGGTGGAATGATGTTC
FV_MYB46RTF3	GAAAACATGATTGGGGTTGG
FV_MYB46RTR3	GCCGGGATCACAAATTAGAA

FV_MYB46RTF4	GTGGGACTTGGAGGATCTGA
FV_MYB46RTR4	CCAGTCTTGATCGAGGAAACA
FVOd1 F	CTCGYCYYGGAAATAGGTGGTC
FVOd1 R	CGATTCCCATCCTAAGCAACT
FVOd1-2 F	AAATGGCCAGTGTTGCTGGA
FVOd1-2 R	TCTCTTCAAGTCGGGACGGA
FVOd1L F	AGTCTTGGCAATAGGTGGTCA
FVOd1L R	GACTTGTTTTTGGAGAGGCACA
FVOd1L-2 F	GAAACGCCTTGTGAAGCCAA
FVOd1L-2 R	TTCAACGTTAGCATCGGCCT
FvPecLy1-JRTF	GACATGAGTATCCGCAACAGCAC
FvPecLy1-RTR	CACAACGCCAGCAATCATCAATG
FvPGIP1-RTF	CCTAGTTCATACGGGAAATTCGTTG
FvPGIP1-RTR	TTCATGTTAGCAAATGAGGTTGGG
FvPR1-F	CCTCATTTCCCTCGTAGCCTTAGCC
FvPR1-R	CTTTGTGCATAGGCTGCTAGATTGGG
FvPR4-RTF	CGAGGACAACAACTGGGATTTG
FvPR4-RTR	GTCACTAGCAGACATTTTCCACAGG
FvPR5.3F	ACCTCCTAATGACACTCCCGAAACA
FvPR5.3R	CGTAGTTAGGTCCACCGAAGCATGTA
HindIII_flank_2F	GTCCGATTGGAAGCAAGAAC
LB_Nested_2_R	GAGAGGCGGTTTGCGTATTG
PPT-F2n	TCCACGCTCTACACCCACCT
PPT-R2n	AGAAACCCACGTCATGCCAG

2.7 Enzymes

Equipment	Supplier
DNase I	Thermo-Fischer Scientific, Waltham, MA, USA
iScript Advanced Reverse Transcriptase	Bio-Rad, Hercules, CA, USA
Platinum ® Taq DNA polymerase	Thermo-Fischer Scientific, Waltham, MA, USA
SsoAdvanced™ Universal SYBR ® Green	Bio-Rad, Hercules, CA, USA

2.8 Size marker ladders for gel electrophoresis

Ladder size	Supplier
100 bp	New England BioLabs, Ipswich, MS, USA
1 kb	New England BioLabs, Ipswich, MS, USA

3 Methods

3.1 Locations:

Most laboratory experiments were conducted at NIBIO (Norwegian Institute of Bioeconomy Research) at the Division for Biotechnology and Plant Health in Høgskoleveien 7, Ås, Viken, Norway (59°39'58.8"N 10°46'26.8"E). Experiments related to microscopy of cell walls were carried out at the NIBIO Division of Forestry and Forest Resources at Høgskoleveien 8. Plants for the experiments were grown at SKP (Senter for Klimarelatert Planteforskning) at Kirkeveien 16 in Ås.

3.2 Maintenance of plants:

Gene editing using CRISPR/Cas9 for a deletion in *Fragaria vesca-MYB46* (*FvMYB46*) was performed prior to my involvement. Leaf discs of *F. vesca* H4X4 were transformed using the vector pCas9-TPC in *Agrobacterium tumefaciens.* Two sgRNAs were used for cutting at two different sites separated by 81 bp of the *MYB46*-gene. Each of the sgRNAs were expressed using a FvU6-26 promoter optimized for *F. vesca* (Tage Thorstensen, unpublished). Putative transformants were selected on MS (Murashige & Skoog) media containing 3 mg/mL BASTA. 47 plants (primary transformants, T0-generation) had been verified as successfully edited using PCR with primers flanking the two gRNAs and gel electrophoresis showing an 81 bp deletion ~compared to WT (wild-type). PCR-products were furhter cloned and sequenced which confirmed a 81 bp deletion in *MYB46*. An additional 3 plants were positive for the BASTA resistance cassette, but had no presence of Cas9 and no deletion in *MYB46,* suggesting a partial deletion of one or more T-DNA during the transformation event (NIBIO, unpublished). The three additional plants were used as control plants for most parts of this study, and are referred to as *B-plants* (B= "big";initially, they appeared much bigger in size than the *myb46* transformants) or *internal controls* in this study.

Plants of around 5 cm height were moved from MS/Basta culture to soil, and maintained in a growth chamber at SKP. The growth conditions were: 18 °C and 16 hours lighting, relative humidity around 75 % and a CO_2 concentration of 400 ppm (parts per million). After 4 weeks,

stolons were cut and transplanted as new individual plants. This generation is here referred to as V1 (V for *vegetative*), while the mother-plant generation; the primary transformants and the 3 control plants, is referred to as T0. Transplantation of V1 was done regularly to ensure available plant material of correct age for each experiment. Seeds of T0 were surface-sterilized and sown in peat soil. The seed-propagated generation is referred to as T1.

3.3 DNA: Gene verification of putative gene edited plants:

3.3.1 Harvesting

After T0, V1 and T1 plants had grown 3 to 4 mature leaves, leaflets of a selection of the plants were harvested for DNA analysis. Leaves were immediately brought to the laboratory for DNA extraction and isolation, and stored at -20 °C.

3.3.2 DNA extraction and isolation

Plant leaflets of roughly 100 mg were ground to a fine powder in liquid nitrogen using pestle and mortar. For DNA extraction and isolation, the DNeasy® Plant Mini Kit from QIAGEN was used. Beyond the procedure of the standard protocol, the recommended centrifugation of the initial lysate was carried out (step 4 of the protocol).

3.3.3 PCR

The Cas9 cassette, the MYB46 fragments as well as other sequences related to T-DNA inserts were amplified for genotyping using PCR.

Table 3.3.1: *Master mixes for PCR (25µL x the amount of samples used)*

Reagent	Amount
10x PCR-buffer (-MgCl)	2,5 µL
Nucleotides	2 µL
$MgCl_2$	0,75 µL
Primer forward	1 µL
Primer reverse	1 µL
Platinum Taq-polymerase	0,1 µL
Template from sample	1 µL (added to PCR strip)
Distilled H_2O	16,65 µL
Total	25 µL

3.3.4 Gel electrophoresis

Gels were made of TBE buffer and 2 % agarose, with one drop of ethidium bromide for every 50 mL buffer. Wells were loaded with ladders of 1 kb (kilo base pairs) and 100 bp, depending on the expected length of the products. DNA was mixed with 1/6th of 6X Loading Dye. DNA amounts varied, but a minimum of 3 µL of PCR product was applied to each well during all gel electrophoreses.

3.4 Disease phenotypic assays

3.4.1 Harvesting of material:

Leaflets aged 4-7 weeks were harvested, cut at the petiole and brought to the lab for treatment under a laminar flow cabinet. Leaf samples of around 100 mg, 3 for each of myb46 mutant plants and control plants (3x2 =6n) were stored at -80 ºC for gene expression analysis. Fully emerged flowers were cut off at the petiole, 1-2 cm from the floral base, and placed in 9 cm Petri dishes. Petri dishes were prepared with 2 layers of filter paper, and 2 mL of water was added to ensure high relative humidity.

3.4.2 Isolation of fungi:

Fungal cultures of B. cinerea were grafted on Potato Dextrose Agar, and grown at 18° C, for 2-4 weeks under 24-hour lighting before being used. B. cinerea strain Bc. 96/16-8.2, isolated from strawberry in Valle in 2016 (NIBIO) was used for the first detached leaf assays. For all the detached flower assays as well as the final detached leaf assay, strain Bc. 101, harvested from strawberries in Grimstad, 2002 (NIBIO) was used.

3.4.3 Surface desinfection:

Leaves were disinfected by submersion into the following separate liquids for 1 minute each: 1 % chlorine (diluted 4% sodium hypochlorite) 70 % ethanol, distilled H2O (dH2O), and another container with dH_2O. After surface disinfection, leaves were placed on two layers of pre-autoclaved filter paper in 9 cm Petri dishes. 2 mL of dH_2O was applied to the filters, to maintain high relative humidity within the petri dishes.

3.4.4 Inoculum preparation:

PDA plates containing B. cinerea strains Bc. 96/16-8-2 and Bc. 101 aged 2-4 weeks after grafting were flooded with PDB (Potato Dextrose Broth) and scraped using a bacteriological loop. The suspension was sieved through a sterilized spoon strainer, to remove remains of mycelium and agar. An amount of Tween® 20 was added, up to 0,1 % concentration, to ensure even distribution of the conidial suspension. The amount of conidia was estimated using a Bürker haemocytometer. The concentration was adjusted to 105 conidia/mL for detached leaf assays, and 0.5x105 conidia/mL for detached flower assays.

Table 3.4: *An overview of the two genotypes and the two types of treatments given in detached leaf assays, detached flower assays and microscopy.*

Genotype	Mutant (*myb46*)		B-plant/internal control	
Treatment	**Mock-inoculated**	**Inoculated**	**Mock-inoculated**	**Inoculated**

3.4.5 Inoculation:

Inoculation was carried out with basis on (Audenaert et al., 2002). Leaves were wounded prior to application of spore suspension, to facilitate pathogenic growth. Wounding was done using a 0.5-10 µL pipette tip with force applied in a downwards, slightly circular motion to ensure puncturing of the leaf. Before each wounding, the pipette tip was filled with 10 µL conidial suspension. After wounding, the pipette was lifted slightly from the leaf, and the drop was released onto the wound. Each leaflet was wounded and inoculated in three spots. For control, a few sets of leaflets were mock inoculated using PDB without spores.

Inoculation of flowers was based on (Rahman et al., 2014). Flower inoculation was carried out by pipetting 10 µL of spore suspension onto the adaxial (bottom) side of the petals. Three different spots on each inflorescence was drop inoculated, adding up to 3x10 = 30 µL per flower. As controls, sets of harvested flowers of both myb46 mutants and control plants were treated with PDB without spores.

Petri dishes with inoculated tissue were sealed using Parafilm. Leaves were incubated at 22° C, 16 hours light/8 hours dark, and flowers in complete darkness by covering with aluminium foil.

3.4.6 Phenotypic scoring of leaves:

Disease assessments of detached leaves were made at 2, 5, and 10 days post inoculation (dpi). For the first few assays, visible lesions were measured in two axes and the mean of the lesion area of the three leaves in each Petri dish was measured. For the final detached leaf assay, lesion diameters were measured using the image analysis software ImageJ. At 48 hours post inoculation (hpi), 3 leaflets of myb46- and control-plants (2x3n) were stored at -80 °C for gene expression analysis.

3.4.7 Phenotypic scoring of flowers

Scoring of flower disease development was carried out based on (Darras et al., 2006). An arbitrary disease severity scale was used, ranking from 0 to 4, where:

0 = no lesions on the petals

1 = 1 to 5 % of petal surface area covered with lesions

2 = 5 to 25 % of petal surface area covered with lesions

3 = 25 to 50 % of petal surface area covered with lesions

4 = 50 to 100 % of petal surface area covered with lesions

The development of disease lesions on flowers was measured at 24, 48, 72, 96 and 120 hpi. A few flowers of all four treatments (4x2 = 8n) (table 3.4) were dissected and fixated for microscopy (section 3.6).

3.5 Gene expression analysis

3.5.1 RNA extraction:

RNA extraction and isolation was carried out on both inoculated and non-inoculated plant leaves. The inoculated material was frozen at -80 °C at 48 hpi, while non-inoculated material was frozen directly after harvest. Homogenization of the material was done using liquid nitrogen in a mortar, and grinding with a pestle.

RNA isolation for the infected leaves was done using Spectrum™ Plant Total RNA Kit (Sigma-Aldrich, St. Louis, MO, USA). However, for the non-treated leaves (section 3.4.1) an alternative approach of lysing of cells was used, a modified protocol for the CTAB-Spectrum method (Wang & Stegemann, 2010).

CTAB-Spectrum method of RNA extraction:

1. PVPP (40 mg/2 mL) was mixed with ß-mercaptoethanol (20 µL/2 mL), and the buffer heated at 60° C for 30 minutes.
2. 900 µL of pre-heated CTAB buffer was added to 100 mg of the ground leaf tissue
3. Mixture was incubated at 60° C with vortexing for 15 minutes.
4. Mixture was centrifuged at 13000 rounds per minute, and the supernatant transferred to a new tube.
5. An equal volume of chloroform:isoamylalcohol mixture (24:1) was added to the supernatant, followed by mixing and centrifugation for 10 minutes at 4° C. After this step, the manufacturer's protocol was followed.

For both RNA isolation methods, protocol A of the Spectrum™ Plant Total RNA Kit was followed, the optional DNase digestion step was carried out once, and elution was performed twice. RNA was finally stored at – 80° C until cDNA synthesis.

3.5.2 cDNA synthesis

cDNA synthesis of isolated RNA was carried out using the iScript™ Advanced cDNA Synthesis Kit for RT-PCR. 200 ng RNA from each sample was used. In the thermal cycling section, the alternate reaction protocol was followed (30 minutes at 42° C and 1 min at 95° C). One sample was made without Reverse Transcriptase enzyme, and one with water instead of RNA sample, both serving as negative controls. After synthesis, cDNA was diluted 10-fold and finally stored at -20 ºC until qPCR.

3.5.3 Identification of homologous proteins:

To identify homologus candidate proteins from *AtMYB46* in *F. vesca*, the Basic Local Alignment Search Tool (BLAST) function in the National Center of Biotechnology Information (NCBI) database was utilized. Specifically the 'pblast' search strategy was used, using standard search parameters. Sequences of high similarity were selected as proteins putatively homologous between *A. thaliana* and *F. vesca*.

3.5.4 Primer design of possible *MYB46*-related genes:

Primers of *MYB-46*-related genes were selected using the 'Pick Primers' function in NCBI's database. Two pairs of primers were selected for each protein-coding sequence. One of each primer pair was selected for an exon-exon junction, and the other pair of primers was selected for localization within the same exon.

3.5.5 RT-qPCR

Reverse Transcriptase – quantitative PCR was performed using the following mixing into 96-well plates:

Table 3.5.1: *Reagents and the amounts used for each qPCR reaction*

Reagent	Amount
Sso Advanced Universal SYBR Green Supermix	10 µL
Forward Primer	1 µL
Reverse Primer	1 µL
cDNA template	2 µL
dH_2O	6 µL
Total amount:	20 µL

3.6 Microscopy of cell walls

3.6.1 Fixation and preparation

Flower stems of all four treatments (table 3.4)(two flowers were harvested for each) used for microscopy were fixated in paraformaldehyde (2%) and glutaraldehyde (1.25%) in Pipes buffer (L-piperazine-N − N'-bis(2-ethane) sulfonic acid buffer, 50 mM, pH 7.2) for 24 h at room temperature, and thereafter in 0.1 M Pipes buffer at 4 °C for more than 24 h.

Tissue sections were made by cutting proximal stems using a razorblade (about 10-20 μm thick sections) and placing on glass slides. These sections were examined with a Leica DMR light microscope at bright field and epifluorescence optics. Images were taken with a Leica camera and software (DFC425/LAS V4.0 020-525-732). Image resolution was 2592 x 1944 pixels. For general observation of tissue morphology, conventional bright field optics were used.

3.6.2 Staining and fluorescence

For examination of lignin-rich tissue, floral proximal sections were stained with Safranine O for 2-5 minutes (Bond et al., 2008). Safranin is a fluorescent dye and the sections stained with safranine were excited at 488 nm and imaged using a BP530 band pass filter (30 nm band width) and an LP590 long pass filter (590 nm). Lignified cell walls appear bright red.

Unstained sections were used for detection of lignin with UV auto-fluorescence, showing blue UV fluorescence of the xylem vessels and the epidermis outer cell walls. Lignin autofluoresces with maximum absorbance in the UV range and requires no dye (Albinsson et al., 1999). Lignin autofluorescence was excited with 488/568 nm radiation and imaged using a BP530/LP590 filter. Lignified cell walls appear bright blue.

For detection of starch grains, the sections were stained with iodine potassium iodide (IKI) (De Neergaard, 1997) which after 1-2 minutes give the starch grains a brownish black color as viewed with bright field microscope.

3.7 Drought stress test

Leaves of T1 at aproximately 2-3 weeks of age were placed in Petri dishes containing 2 Whatman ® filter papers. In each Petri dish, 10 mL of the following concentrations were added: 1) dH_2O, 2) dH_2O, 150 mM mannitol, 3) dH_2O, 300 mM mannitol, with basis from

(Wang et al., 2021). 5 mL were added at first, and another 5 mL were added after 7 days. Leaves were photographed at every 24 hours for 7 days, and evaluated qualitatively.

4 Results

4.1 General phenotypes of primary transformants and B-plants

At the start of the experiment, I received responsibility for maintenance and experiments of 50 CRISPR/Cas9-transformed plants (Tage Thorstensen, unpublished). The transformants were observed regularly, both mutants and interntal controls/B-plants. 47 *myb46* mutant (81 bp deletion in *myb46*) lines and 3 internal controls -B-plants (T0-plants with truncated T-DNA with no Cas9-gene and no deletion in *MYB46*) all confirmed by (Magne Skårn, personal communication), were observed for their phenotypic morphology during growth and development in addition to the experiments conducted. This was to see if there were any obvious differences and thus any off-target effect of the mutagenesis between the two main lines.

The B-plants were, for most experiments conducted in this study, included as controls containing a T-DNA but not a *myb46* deletion; thus presumably being different in their *MYB46* length only. The leaves of the B-plants were shaped less oval than leaves of *myb46* and wild-type (fig 4.1.2). Also, quite importantly for this study, B-plants seemingly developed leaf lesions and aborted their inflorescences more frequently than the *myb46* mutants in the growth rooms without inoculation; however, this was not quantified. Growth was generally slower in B-plants than *myb46* mutants (fig 4.1.1). Slow growth was especially true for stolon-formed clones of the B-plants (V1), which failed to reach sufficient size and development stages for experiments. The availability of fully developed flowers from B-plants for detached flower assays was also limited at each time of the experiments, which made it difficult to properly evaluate the differences in flower susceptibility to *B. cinerea*.

Fig 4.1.1: *Pictures comparing size differences between the internal control plants and myb-46 plants, approximately 3 months after transplantation. General growth was visibly slower or stunted in control plants than in myb46 plants.*

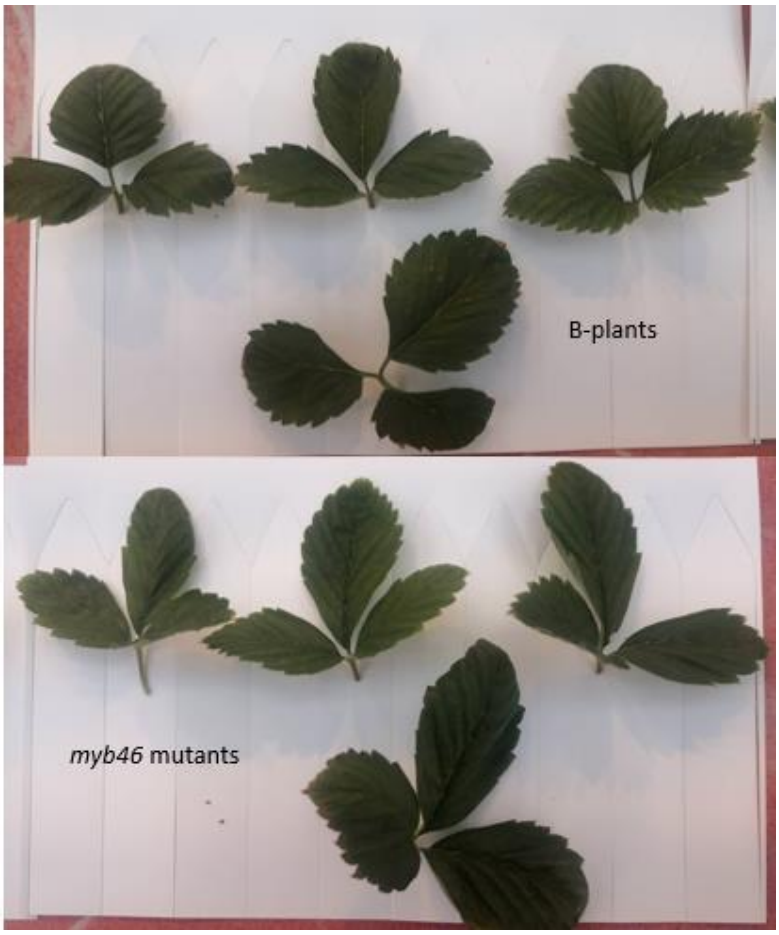

Fig 4.1.2: *Comparisons of the leaf morphology between B-plants/control (top) and myb46 plants(bottom). Notice the B-plant leaves being shaped less oval, and more round.*

4.2 PCR genotyping of putative gene edited plants

4.2.1 T0 genoyping

Gene edited plants (T0), segregated on BASTA medium confirmed for a deletion in *myb46* (Tage Thorstensen, unpublished), were screened for T-DNA insertion sites using inverse-PCR of left borders of T-DNA, followed by sequencing of these regions. Two regions were identified, closely located in the genome. For all the tested *myb46* lines, these product sizes were observed (Inverse PCR data, Magne Skårn). This indicated that the two T-DNAs had the same presence and localization in all plants. The T-DNAs may have been of different lengths, indicating the presence of a truncated T-DNA (Magne Skårn, personal communication) and thus only one copy of Cas9. For practical purposes, primary transformants (T0) of *myb46* mutants were in most cases regarded as the same genotype. Additionally, T0 plants were screened for the presence of BAR (fig 4.2.1), rendering the plants tolerant to BASTA medium. BAR was present in all lines tested (n=10) (more lines were screened earlier by Magne Skårn).

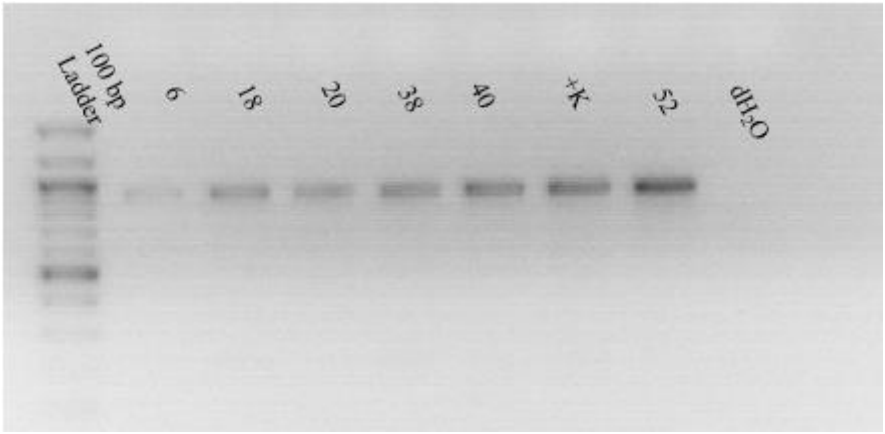

Fig 4.2.1: *Gel electrophoresis of PCR-reactions on genomic DNA of T0 plants using the primers PPT-F2n and PPT-R2n, for the presence of BAR in both the mutants and the internal control plants (B) of T0. Expected amplicon size = 915 bp. Genotype 6, 18, 20, 38 and 40 are myb46 lines, while 52 is an internal control (B) plant. +K is a purified plasmid prep designed for the T-DNA cassette, acting as a positive control.*

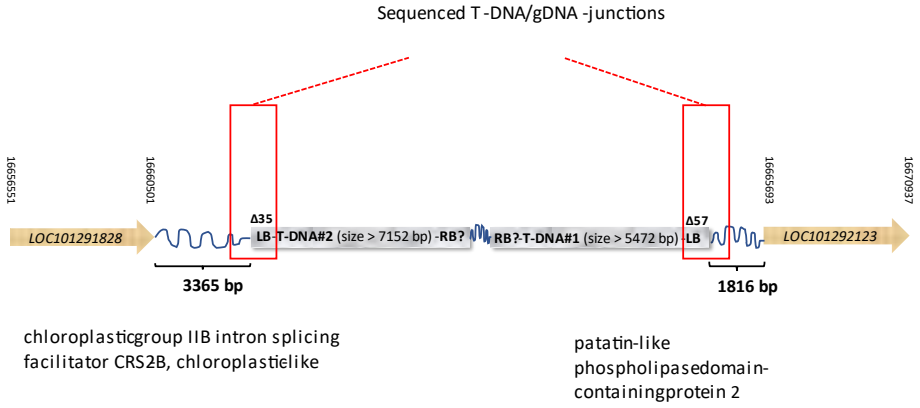

Fig 4.2.2: *Overview of the inverse PCR procedure used in this study (Inverse PCR data, Magne Skårn). Simply put, known border sequences of the T-DNA were used to synthesize DNA away from the borders. DNA formed a ligated circular molecule by use of certain enzymes. These circular regions were sequenced to find their localization in the genome. By amplification of a junction between T-DNA and a known region (fig. 4.2.6, 4.2.7), the localization is confirmed. Figure by Magne Skårn, NIBIO.*

4.2.2 Genotyping V1

Out of the 50 primary transformants, a set of V1 plants (n=22) (vegetatively formed from runners from the *myb46*- and B- T0-plants) were selected for verification of the Cas9-cassette and *myb46*. Genotyping of V1 was done to see if *myb46* and Cas9 were inherited clonally or

if somaclonal variation occurred in these lines. Of the 50 primary transformants, 22 daughter plants (V1), each from different primary transformants, were analysed for genotyping. For V1 lines tested (n(*myb46)* = 19; n(B) = 3) by PCR-genotyping with FVMYB46 F and FVMYB46 Rseq2, a deletion in *MYB46* was inherited by daughter plants (V1) of *myb46* mutants (n=19), while no deletion in *MYB46* was detected in V1 of B-plants (n=3) (fig 4.2.3). Expected band size for plants with deletions in *MYB46* were 162 (fig 4.2.3), and without deletions 243 bp. For the Cas9-genotyping (Cas9 F3n and Cas9 R3n), all V1-*myb46* lines tested (n=19) gave the same expected PCR-product of 304bp as their mother-plants; the B-plants showed no bands (fig 4.2.3) All lines tested thus showed the same length of *MYB46* and presence/absence of Cas9 as their clonal originator.

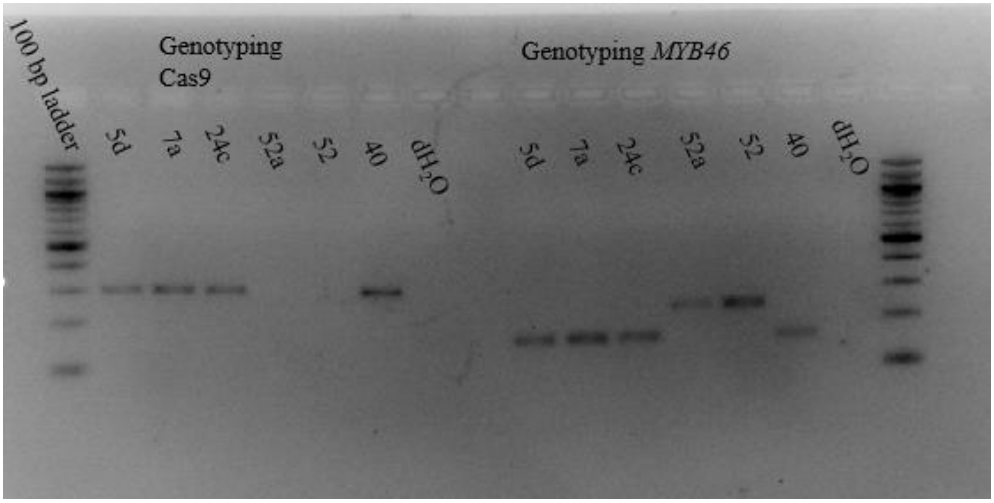

Fig 4.2.3: *Gel electrophoresis of PCR-products from genotyping genomic DNA fromV1 plants using primers Cas9 F3n, Cas9 R3n, FVMYB46 F and FVMYB46 Rseq2. A letter after the initial number denotes a V1-plant. 52A is a control V1 plant, from a runner of the internal control plants. 40 is a T0-myb46 plant, and thus control for a deletion in MYB46. 40 is also a positive control for the Cas9-insert.*

Table 4.2.1: *An overview of the mother-plants (T0) that have been confirmed to maintain alleles of Cas9 and MYB46 in the next clonally propagated generation (V1). (B) Denotes a B-plant. (Continues next page.)*

Working ID #	
1	38
4	39
5	40

6	41
7	42
18	43
20	44
22	45
29	46
31	47
35	48
36 (B)	52 (B)
37	53 (B)

4.2.3 Genotyping T1:

To verify the assumed copy number of T-DNAs (2) from the inverse PCR (Magne Skårn) and to identify plants with mutation and no cas9 insertion, a total of 24 plants propagated from seeds in peat soil from 3 primary transformants: (T0) Working ID #43, #44 and #45 were maintained for bioassays. These sexually propagated plants were genotyped for deletions in *MYB46* as well as segregation of Cas9.

The T1 plants (n=24)(sexually produced from T0) were genotyped using the same primers as for V1. Here, Cas9 was expected to be segregated out for some (25 %) of the mutant lines, due to Cas9 being a hemizygous allele; however, if the copy number of Cas9 indeed exceeds 1, this segregation was not to be expected. The goal of this was mainly to identify lines without Cas9, only containing the *myb46* mutation.

PCR-genotyping using FVMYB46 and FVMYB46 Rseq2 (fig 4.2.4) for 23 of the plants gave a PCR-product of ~160bp suggesting that these plants carried the same deletions in *MYB46* as their respective parental line. Surprisingly, plant #43_T1_16 (fig 4.2.4b) gave a product of ~240bp, suggesting that it did not contain a mutation.

Presence of Cas9 was screened (fig 4.2.5) using primers: Cas9 F3n and Cas9 R3n. 12 of the 24 analysed plants did not give any Cas9 products, while the remaining 12 did. 43_T1_16, which exhibited a non-deletion in *MYB46* did not show presence of Cas9.

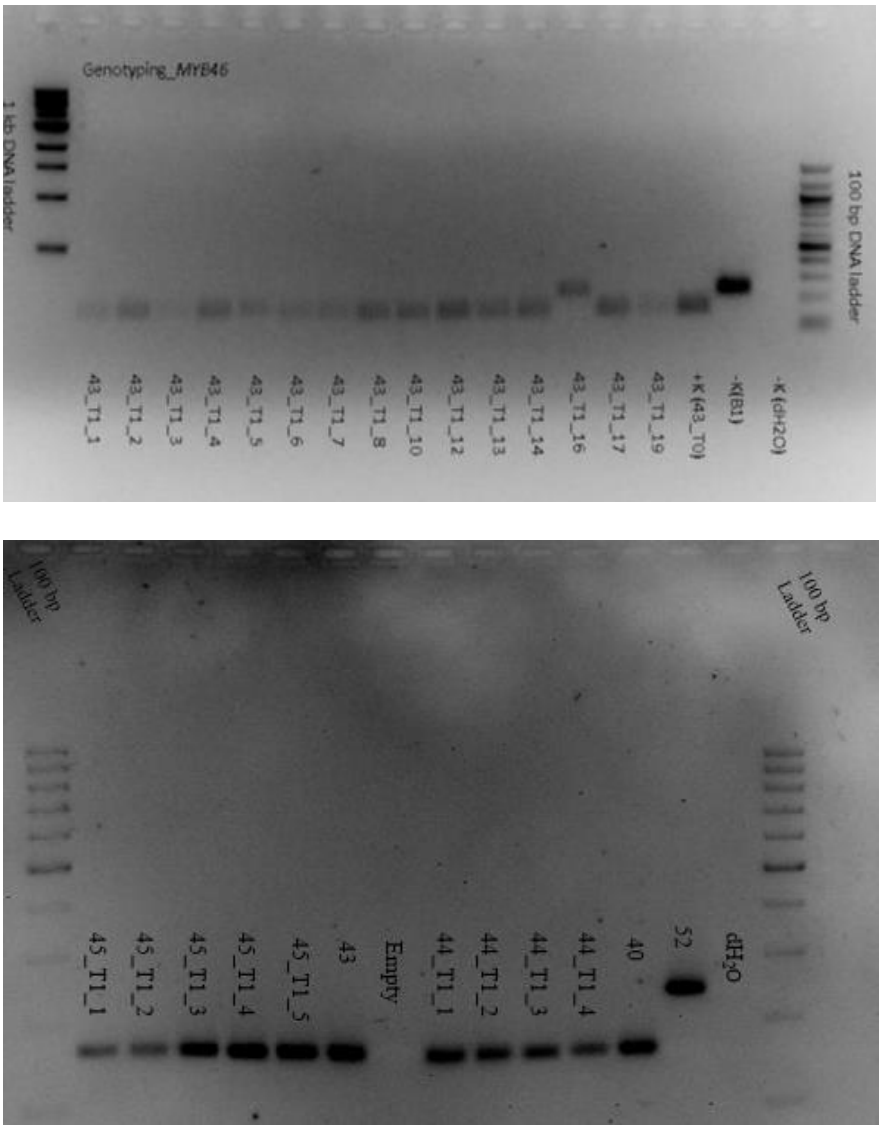

Figure 4.2.4 a) and b): *Gel pictures from T1 genotyping of MYB46 length using primers* FVMYB46 *and* FVMYB46. *Genotype 43(T0) was included in b) to verify that 43_T1_16 indeed originated from a myb46 mutant. a) by Magne Skårn, NIBIO.*

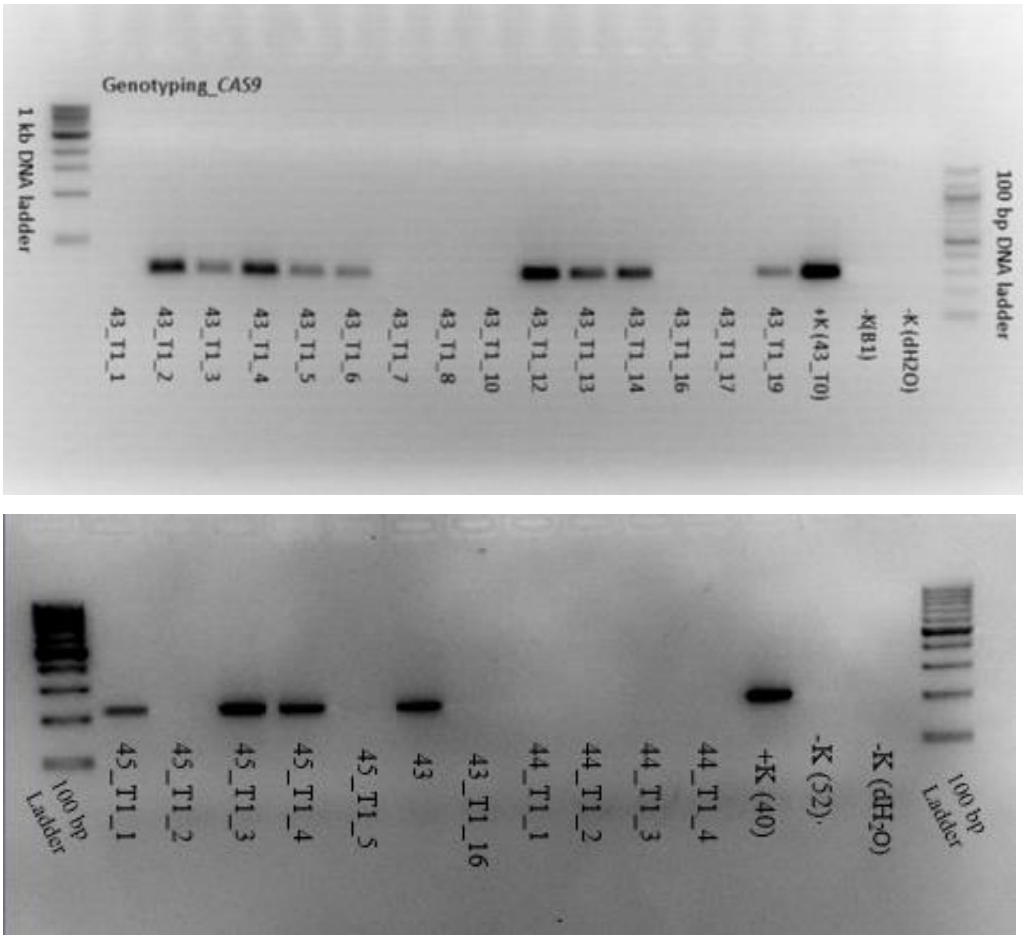

Figure 4.2.5 a) and b): *Gel pictures from genotyping of Cas9 in T1. 43_T1_16 is included in both figures, while 43 (T0) is included in b). a) by Magne Skårn, NIBIO. It should be noted that 45_T1_2 (fig b) did show a weak product of T-DNA flanks of the Cas9 cassette, which could mean that a truncated T-DNA was present here. See fig 4.2.6 b) and 4.2.6 b) for of 45-2.*

Although not a primary objective in this study, the segregation of Cas9 in T1 progenies was tested to investigate possible copy numbers. Since T-DNA insertions in general are inserted as hemizygous alleles, the expected inheritance of Cas9 in the T1 generation was 3:1 (Cas9:loss of Cas9) for one-copy insertions, as for a single Mendelian trait. The PCR analysis of the T1 progeny showed a 1:1 ratio, assuming that 43_T1_16 actually comes from a *myb46* mutant seed, and that 45_T1_2 does not have the Cas9 cassette. However, the ratios may have differed, depending on the actual origin of 43_T1_16 and genotype of 45_T1_2. Although only 24 individuals were observed, a Chi-square test was carried out for all combinations of assumptions to observe the likelihood of the observed frequencies, assuming no effect on germination rate and seedling lethality; moreover, a single-copy of Cas9 must be assumed. A *p*-value less than 0.05 was selected for testing of deviation from a 3:1 segregation.

Table 4.2.2: *Genotype frequencies of Cas9 and lack of Cas9 (-Cas9) in the 24/23 samples of the T1 progeny, and the estimated probability (p) of the observed frequencies based on the values of a Chi-square test table. One degree of freedom (df) was applied.*

Assumptions	Cas9	-Cas9	Total	**Ratio (Cas9: -Cas9)**	Chi-sq value	**Estimated *p* (df=1)**
With 43_T1_16	12	12	24	**1:1**	3	**0.1 >*p*>0.05**
Without 43_T1_16	12	11	23	**12:11**	2.505	**0.2>*p*>0.1**
With 43_T1_16 and Cas9 in 45_T1_2	13	11	24	**13:11**	2.27	**0.2>*p*>0.1**
Without 43_T1_16 and with Cas9 in 45_T1_2	13	10	23	**13:10**	1.806	**0.2>*p*>0.1**

Based on probability, there is not strong enough deviation in the observed segregation values to conclude that Cas9 does not segregate 3:1 (Cas9: no Cas9) in T1.

4.2.4 Genome Localization of Cas9 in T1-plants:

The same T1 plants that were screened for *myb46* deletions and Cas9 presence were also tested for genome localization of Cas9 in the known regions flanking the T-DNA (fig 4.2.6 and 4.2.7), based on inverse PCR data (Magne Skårn).

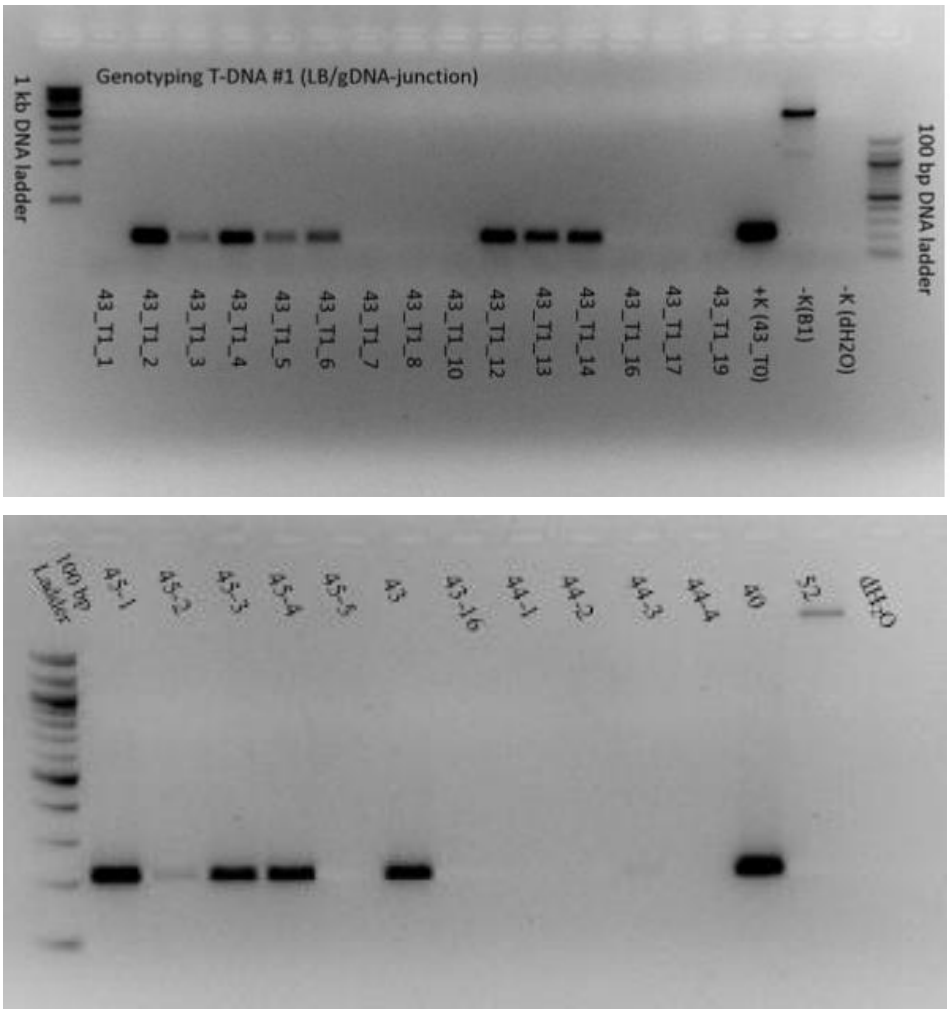

Fig 4.2.6 a) and b): *Genotyping of the T1 plants' T-DNA localization using primers HindIII_flank_2_F and LB_Nested_2_R, designed for a left border- genomic regionjunction. Notice 43_T1_19 (a) which is negative for this junction while being positive for Cas9; however, it may be a false positive due to its weak band and the well being adjacent to a positive control (4.2.5b). Interestingly, B1 and 52 show bands greater than 2kb, which is likely to be an unspecific binding. Expected amplicon size: 217 bp. Figure 4.2.6 by Magne Skårn, NIBIO.*

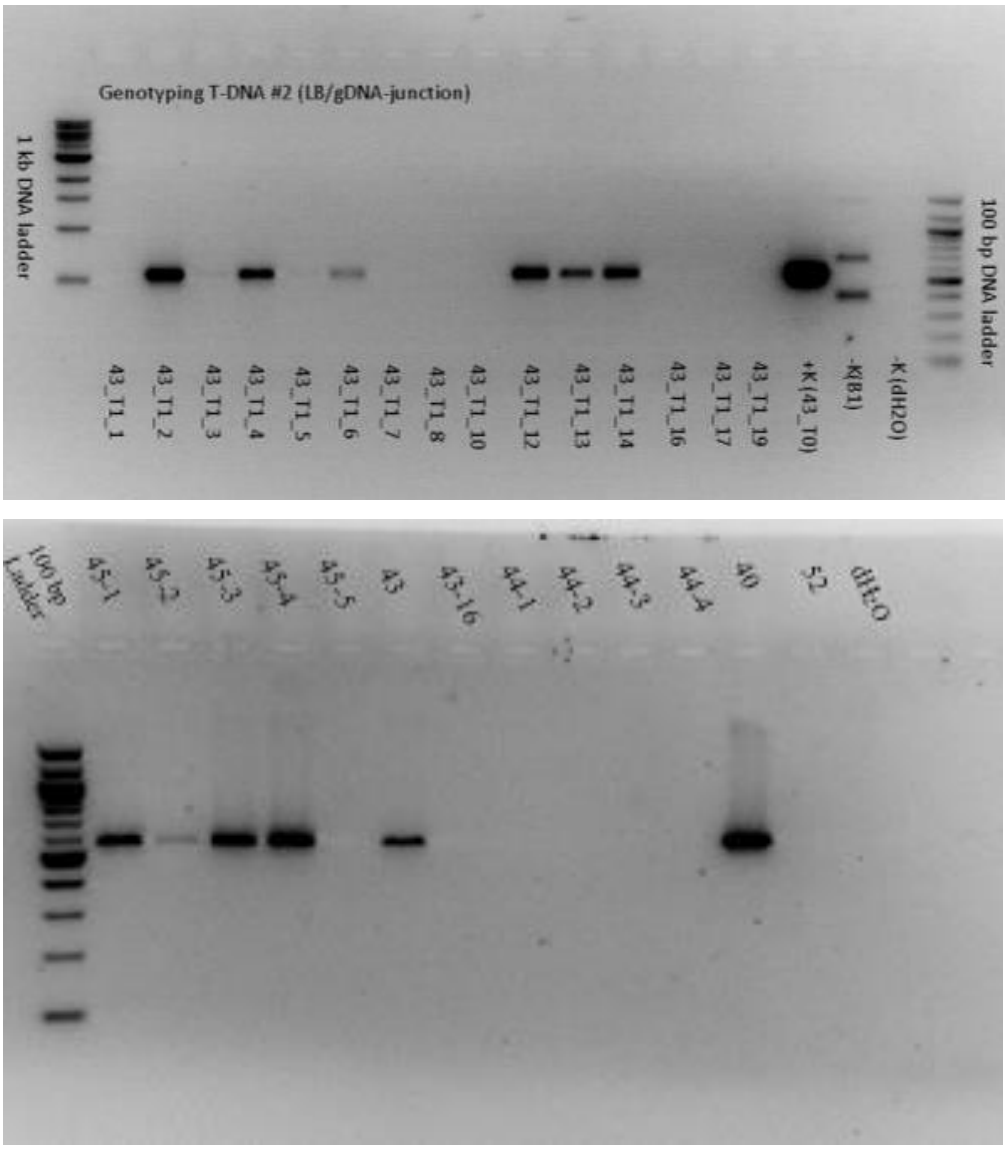

Fig 4.2.7 a) and b): *Genotyping of T1 plants using primers Flank_upstream_T-DNA2_2_F and LB_Nested_2_R, designed for a T-DNA left border – genomic region junction. Notice 43_T1_19/43-19, which is negative for this junction also. Expected amplicon size: 571. Fig a) by Magne Skårn..*

The Cas9-specific left border-known genomic region junctions for genotyping showed that all genotypes that were positive for Cas9 were also positive for the known T-DNAs, apart from 43-19 (fig 4.2.7b). This could indicate that Cas9 is located elsewhere in this specific plant's genome, assuming that it is not a false positive for Cas9.

4.3 Bioassays for determination of disease resistance

4.3.1 Detached leaf assays

To test whether T1-*myb46* mutants (without T-DNA) were more resistant to *B. cinerea* infections than WT, detached leaf assays were performed. These assays were carried out a total of four times, as the assay procedure requires optimization with respect to the specific

tissue and fungal pathogen. In the first two assays, strain Bc. 96/16-8.2 (harvested from strawberries in Valle, 2016) was used for inoculation, while Bc. 101 (harvested from strawberries in Grimstad, 2002) was used in the final two. In the first assay, a concentration of 10^6 CFU/ml was used, as in (Audenaert et al., 2002). In this assay, the leaves developed lesions after 24 hours, and were more or less covered by lesion area after 48 hours, much quicker than expected. To simulate a less intense pathogenic pressure, the concentration for the remaining assays was reduced to 10^5 CFU/ml. For calculation of leaf lesion area, a ruler was used to measure the lesion diameter in two axes for each of the inoculated leaves. In the fourth and final assay, ImageJ was used to get an accurate measure of the lesion area as well as leaf size, enabling calculation of relative lesion size (as opposed to just the lesion size). The detached leaf assays leading up to the final one were not used for statistical analysis, but were used for optimization of the methods and testing isolate activity; based on these measurements, there were no obvious difference in susceptibility between genotypes. The data in the figures and table in this part of the research are from the final detached leaf assay only.

After the detached leaf assay method had been established and the concentrations and activity of the pathogenic isolates had been tested on the V1 and T0 plants, 22 leaflets of homozygous *myb46*-knock out plants without Cas9 (fig 4.2.5) and 18 leaflets of WT *F. vesca* H4X4 plants were inoculated with *B. cinerea*. 6 leaflets from each of the genotypes were mock-inoculated to serve as negative controls (table 4.3.1). No infection was observed in any of the mock-inoculated leaflets. At 2 dpi, no infection was observed in any but one of the inoculated leaflets (fig 4.3.1, fig 4.3.2), and as such lesion area at 2dpi was not used for statistical analysis. To avoid statistical noise as a result of unsuccessful infections, an arbitrary threshold of at least 2 % relative leaf lesion area at 10dpi was applied for the calculations. As wounding alone causes small necrotic lesions, this threshold was set. As such, miniscule lesions were ignored for statistical analysis. Consequently, leaflets that did not meet this threshold at 10dpi were not included in the statistical analysis at 5dpi.

In some of the analysed material, lesions appeared along the leaf edges or at the petiole end of the leaves. Where it was possible to distinguish these types of lesions from lesions caused by inoculations, these unintended lesions were not included as part of the relative leaf lesion area.

Table 4.3.1: *Table showing the total leaves and the ratio of successful and unsuccessful infections for the different treatments. MI = mock-inoculated*

Genotype/Treatment	Total leaves	Ratio successful:unsuccessful infections
myb-46/inoculated	22	18:4
WT/inoculated	18	16:2
myb-46/MI	6	0
WT/MI	6	0

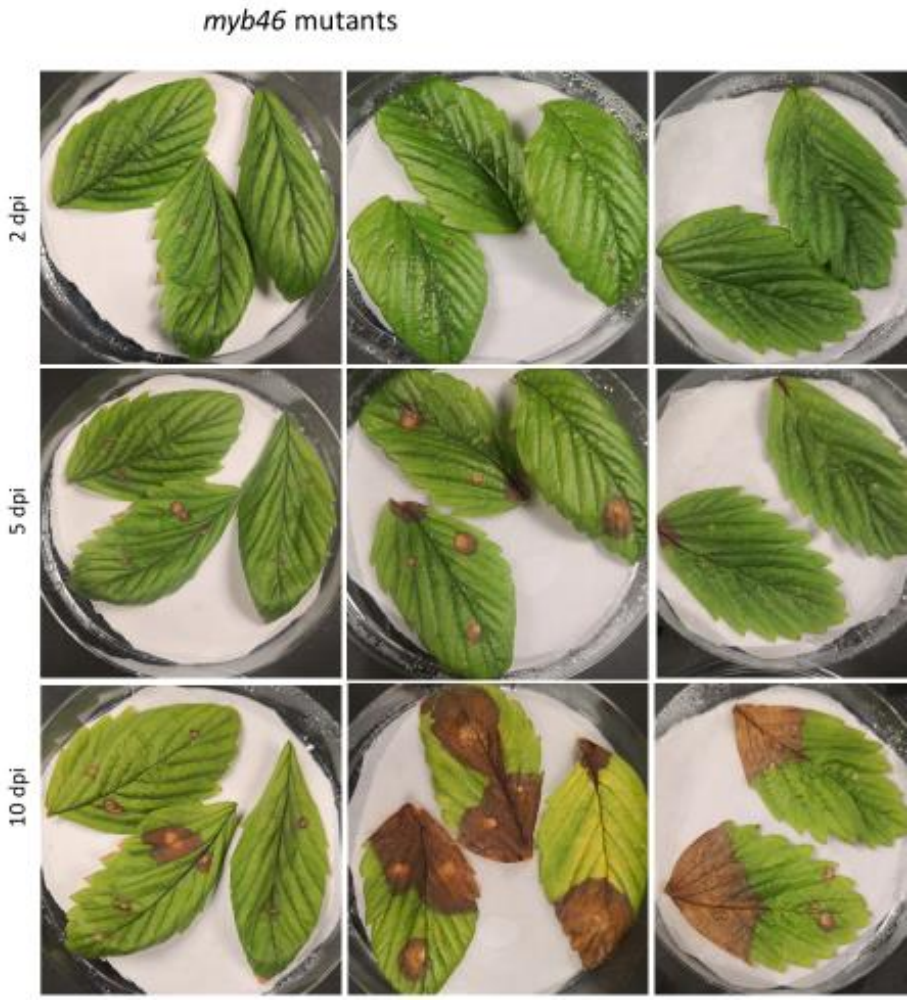

Fig 4.3.1: *Leaf lesion development for leaves of myb46 mutants from 2dpi to 10dpi.*

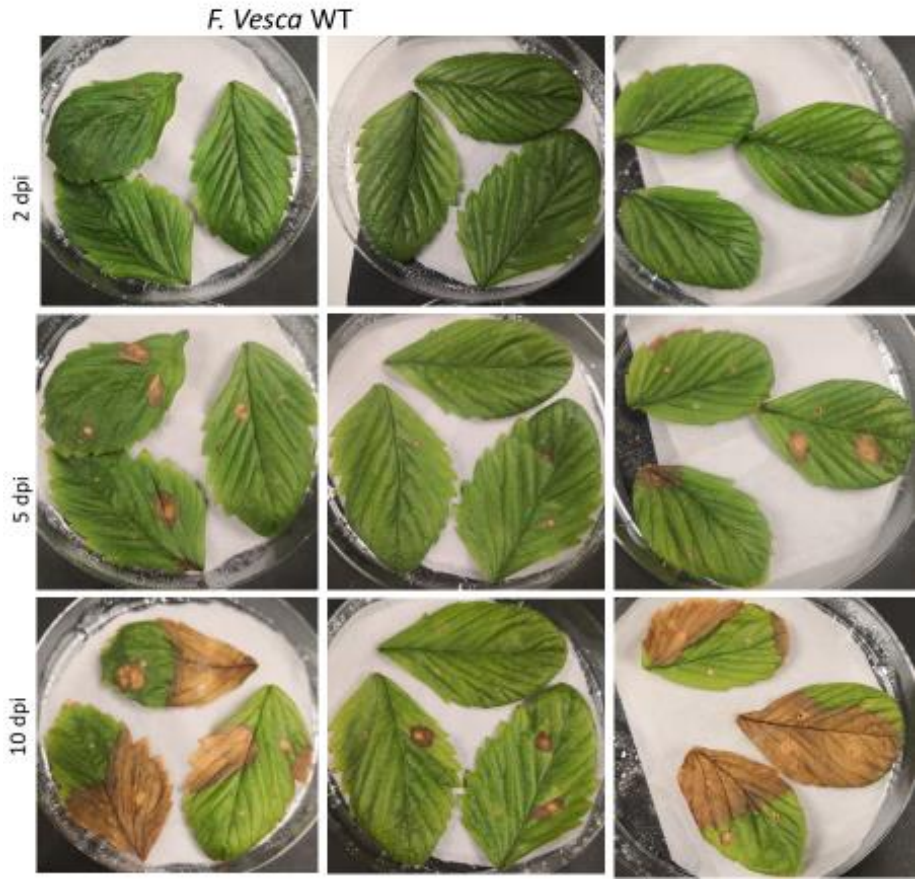

Fig 4.3.2: *Leaf lesion development of leaves of WT-plants from 2dpi to 10dpi.*

Table 4.3.2: *Averages of the relative leaf lesion area (%) of the two different genotypes used, with the standard deviation in parenthesis. Negative controls did not develop lesions.*

Dpi	*myb46*	Wild type
5 dpi	2.67 % (3.17 %)	3.63 % (4.70 %)
10 dpi	32.30 % (30.58 %)	32.11 % (24.53 %)

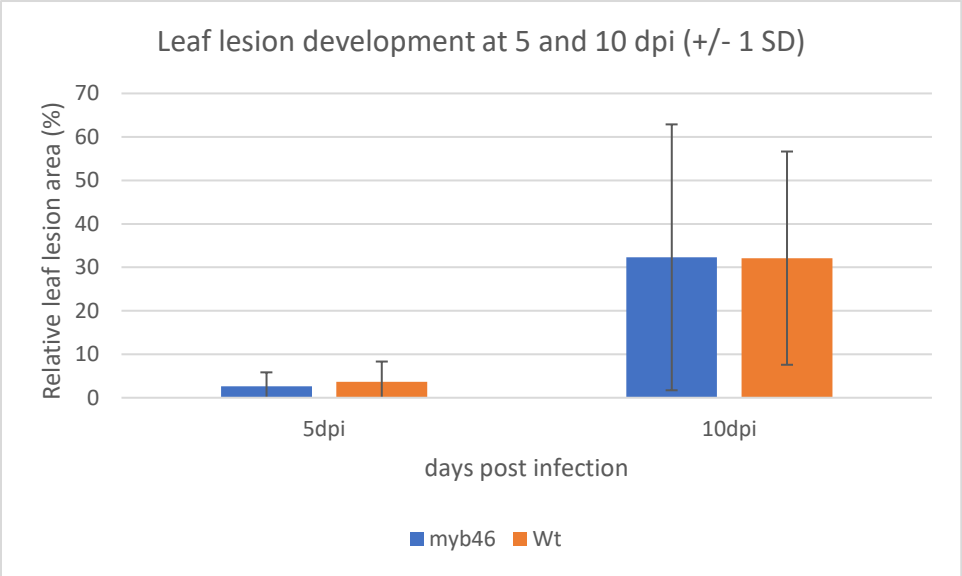

Fig 4.3.3: *Bar graph showing average relative leaf lesion area (%) +/- 1 standard deviation of the two genotypes at 5 and 10 dpi with B. cinerea isolate Bc. 101.*

The detached leaf assays showed similar average values of relative leaf lesion area for *myb46* (32,3%) and wt (32,11%), especially at 10 dpi (table 4.3.2 and fig 4.3.3). At 5 dpi, *myb46* plants displayed slightly lower relative leaf lesion area (2,67%) than WT (3,63%). Importantly for the statistical analysis, the standard deviation of all average values were high (fig 4.3.3), suggesting a high variance and thus inconsistency between the lesion development of all treatments. The data in this experiment do not provide any evidence suggesting that leaves of *myb46* mutants are more resistant to *B. cinerea* than leaves of *F. vesca* WT-plants.

4.3.2 Detached flower assays

To test whether flowers of *myb46* mutants (T0) had higher resistance to *B. cinerea* than flowers of B-plants (T0), detached flower assays were carried out. Because of a limited number of control plants and consequently limited amount of available flowers at the right stage at any given time, detached flower assays were done several times. A total of four detached flower assays were carried out. Due to restrictions imposed by the government as part of the 2020/21 COVID-19 pandemic, two of these assays were not completed; thus data from these were only used for observations of trends. A total of 165 flowers, in which 143 were from *myb46* mutants and 22 from internal control (B) plants were assessed for disease development during incubation after inoculation at 24 hour intervals. At each performed assay, a small number of flowers were mock-inoculated (MI) to serve as negative controls. The flowers were observed at 0, 24, 48, 72, 96 and finally at 120 hpi, and disease development (Fig 4.3.4) scored between 0 and 4 as in (Darras et al., 2006).

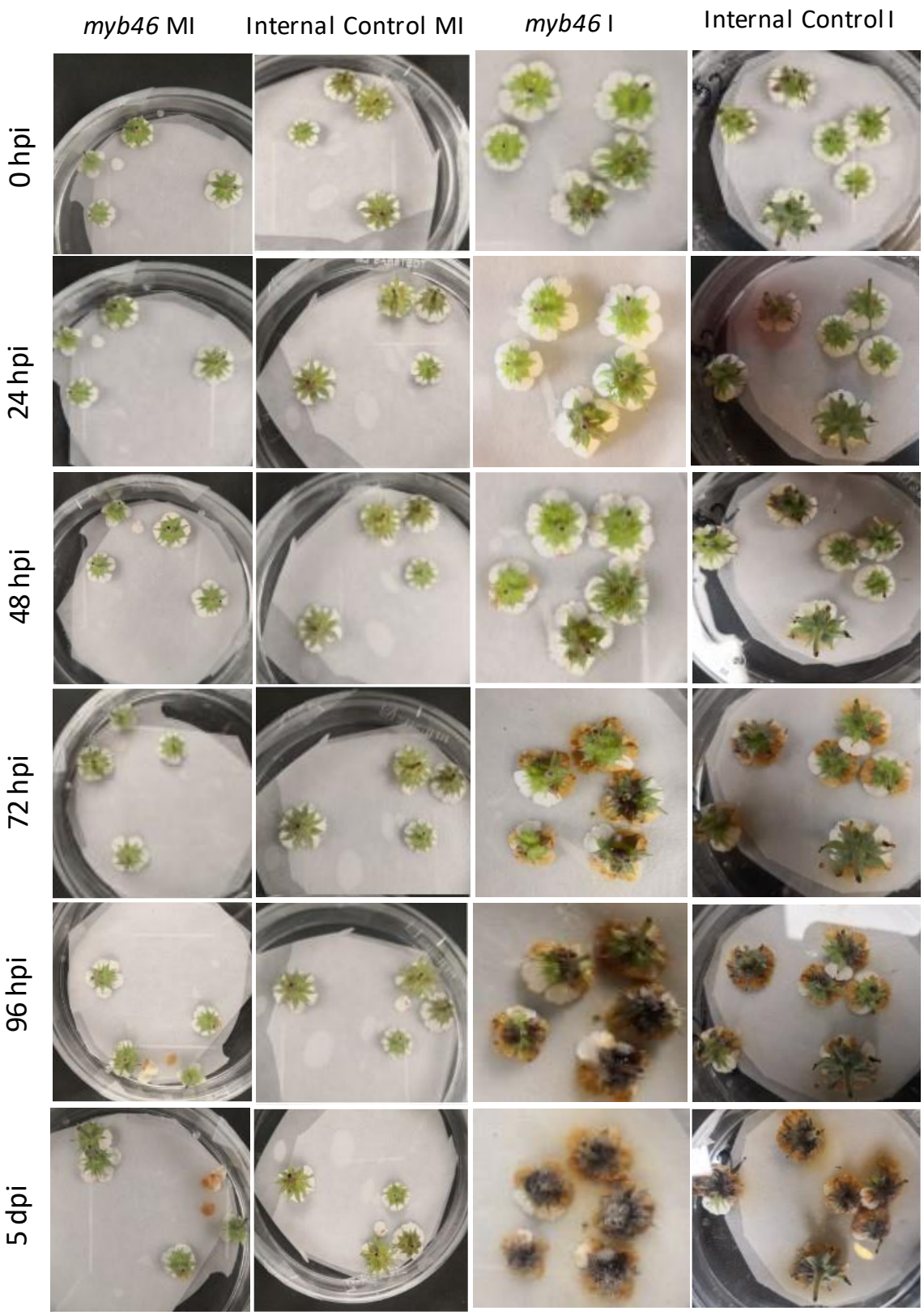

Figure 4.3.4: *Representative disease development for the detached flower assays from 0 hpi to 5 dpi. MI= Mock-inoculated, I= inoculated.*

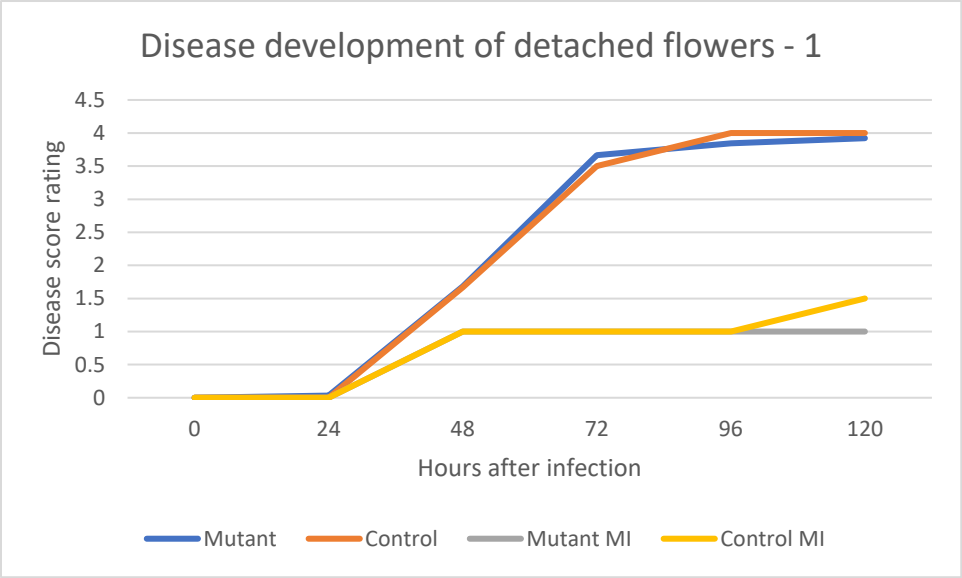

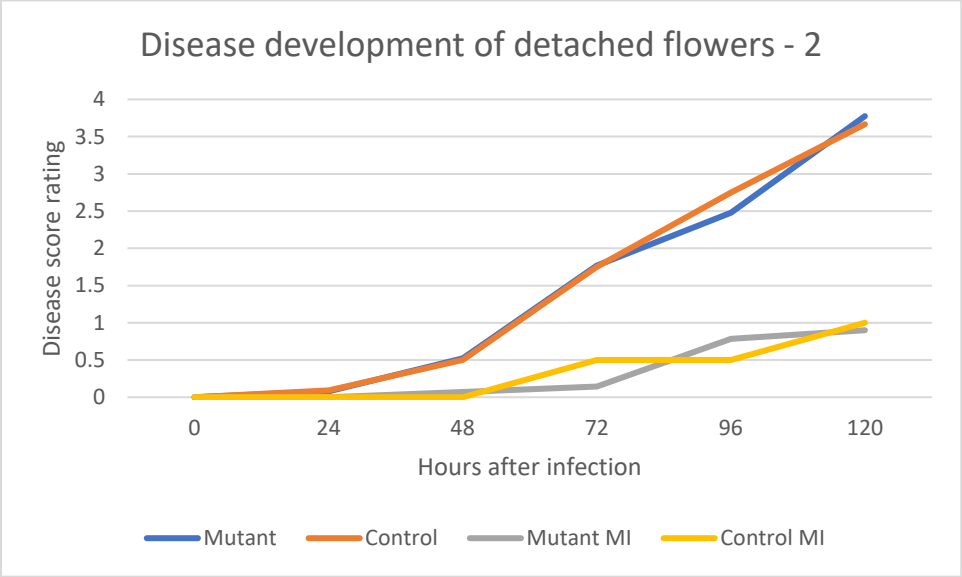

Figure 4.3.5 a) and b): *Tables showing the disease development of the detached flower assays. The two graphs are made separately from each of the separate experiments. The data show the increase in disease score rating from 0 hpi to 120 hpi(5 dpi). MI= Mock-inoculated*

The detached flower assays performed in this experiment did not show any clear differences in susceptibility to *B. cinerea* between the *myb46* plants and the control plants (fig 4.3.5). The two different plant lines showed similar disease development. At 24 hpi, very few lesions were seen; most flowers showed no symptoms of infection. At 48 hpi, most inoculated flowers had visible lesions, covering between 5 % to about 50 % of the petal surface, scored as between 2 and 3 in disease score rating. At 72 hpi, most flower petals were covered by 25 % to about 75 % lesions, between 3 and 4 disease score rating. At 96 hpi, the lesion surface on all inoculated flowersmade up between 50 % and 100 % (4 disease score rating), and even

non-inoculated flowers exhibited lesions, indicating a degree of pathogenic presence in the growth rooms. At 5 dpi, most of the petal surface on all inoculated flowers were covered by lesions, and sporulation was even observed on some of the inoculated material.

Based on the detached flower assays, there is no data suggesting that flowers of *myb46* mutants are more resistant to *B. cinerea*.

4.4 Gene expression analysis

4.4.1 RT-qPCR

To determine the role of *FvMYB46* in the regulation of genes induced by *B. cinerea* infection, infected and non-infected *myb46* and WT *F. vesca* plants were analyzed with qPCR using primers from (Badmi et al., 2019)(table 4.4.1). Additionally, putative direct targets of *FvMYB46* were selected for qPCR, based on homology to genes known to be directly regulated by the *Arabidopsis thaliana MYB46* homolog (table 4.4.3). Lastly, expression of *MYB46* was also quantified (fig 4.4.1). qPCR of pathogenesis-related genes were carried out on infected and non-infected material of *myb46* plants and B-plants. Non-infected material was frozen for RNA isolation right after harvest. Infected material was harvested and isolated 48 hours after inoculation with Bc 101. For *myb46* mutants, working ID plant #3 was used, and for B-plants, #53 was used. For the genes *Odorant1* and *Odorant-like 1*, no cq (quantification cycles) values were observed during qPCR; therefore, they were omitted from graphical presentation. For each treatment, biological triplicates (n=3) or duplicates (n=2) were analyzed to calculate the mean expression. All qPCR cycles were run in two technical replicates. The housekeeping gene *FvEF1α* was used as a control gene, and expression values calculated using the delta-Ct method (Pfaffl, 2001).

Table 4.4.1: *Primers used in qPCR-expression analyses. See table 2.6 for oligo sequences.*

Gene	Primer pair (s)
MYB46	FV_MYB46RTF3 FV_MYB46RTR3 FV_MYB46RTF4 FV_MYB46RTR4
PR1	FvPR1-F FvPR1-R
PR4	FvPR4-RTF

	FvPR4-RTR
PR5.3	FvPR5.3F FvPR5.3R
PGIP1	FvPGIP1-RTF FvPGIP1-RTR
BG2-3	FvBG2-3RTF FvBG2-3RTR
PecLy1	FvPecLy1-JRTF FvPecLy1-RTR

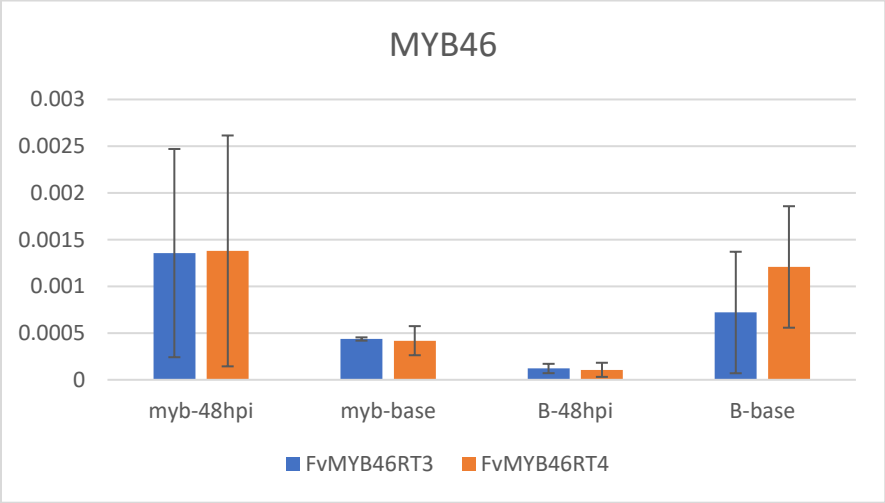

Fig 4.4.1: *Average relative expression values (delta-Ct) (+/- 1 standard error) for MYB46 in F. vesca leaves. myb-48hpi and B-48hpi are myb46 mutants and B-plants, respectively, 48 hours after inoculation. myb-base and B-base are myb46 mutants and B-plants isolated right after harvest.*

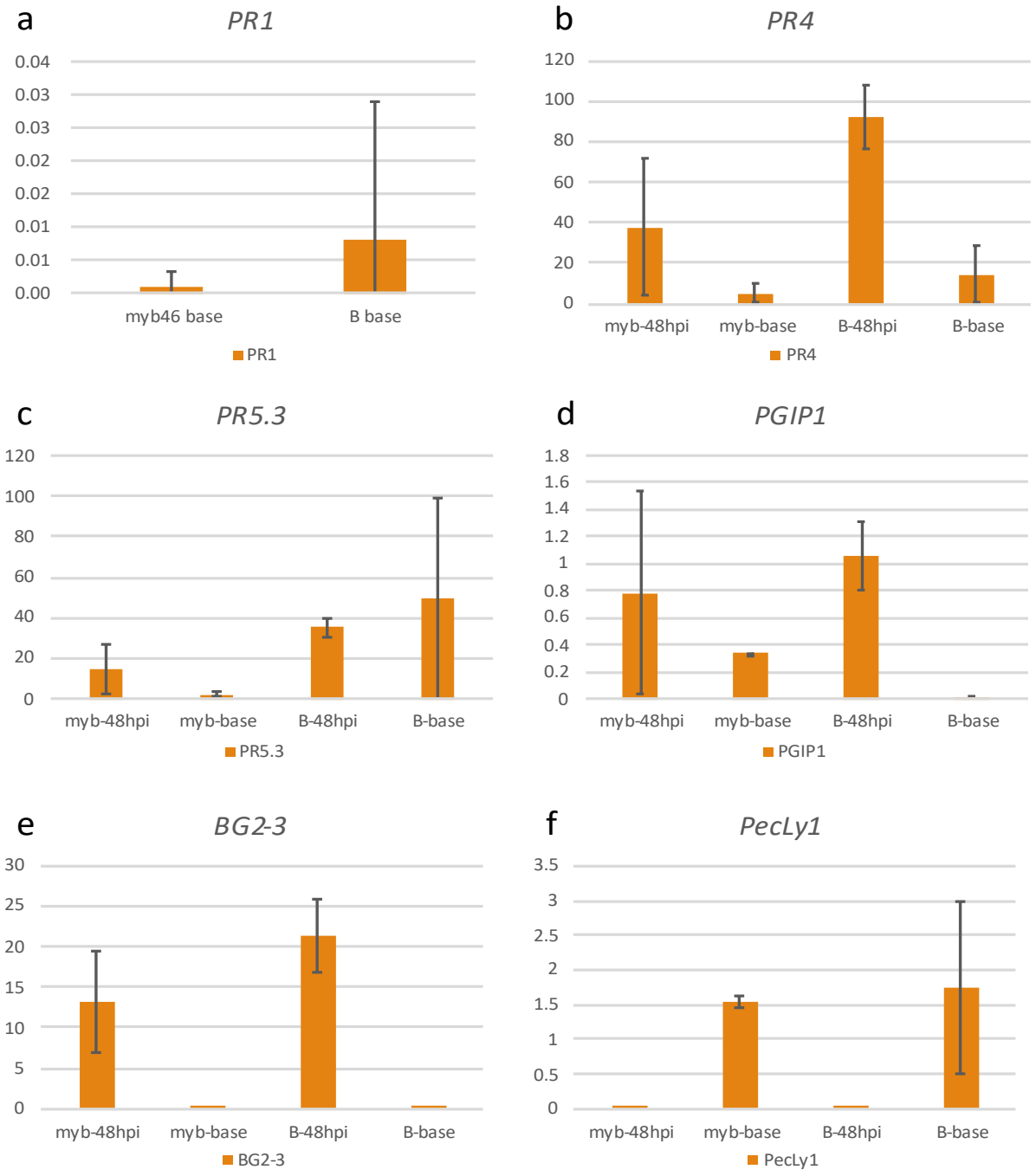

Fig 4.4.2: *Average relative expression values (delta-Ct) (+/- 1 standard error) for pathogenesis-related genes in F. vesca leaves. myb-48hpi and B-48hpi are myb46 mutants and B-plants, respectively, 48 hours after inoculation. myb-base and B-base are myb46 mutants and B-plants isolated right after harvest. a) PR1, b) PR4 c) PR5-3 d) PGIP1 e) BG2-3, f) PecLy1. PR1(a) was not expressed in inoculated leaves.*

Expression levels of *MYB46* were low in all treatments. However, expression of *MYB46* in *myb46* mutants seemed upregulated after infection. B-plants, on the other hand, exhibited lower expression after infection. (fig 4.4.2)

PR1 was expressed in low amounts in untreated plants only (fig 4.4.1a). Expression of *PR4*, *PGIP1* and *BG2-3* (fig 4.4.2 b, d, e) seemingly increased greatly 48 hours after inoculation. *PR5.3* expression increased in *myb46* mutants at 48 hours after inoculation, however for B-plants, non-inoculated materials showed great expression of this gene (fig 4.4.2 c). Notably, the variation and thus standard error for the expression of *PR5.3* in the tested plants was massive. *PecLy1* expression was reduced after infection with *B. cinerea* (fig. 4.4.2 f).

Table 4.4.2*: Genes related to pathogenesis in F. vesca, and genes related to MYB46 in A. thaliana that were chosen for this study. The pathogenesis-related genes were based on (Badmi et al., 2019).*

Gene ID	**Gene name**	**Full gene names/Protein names**
F. vesca pathogenesis-related genes		
FvH4_2g029 20.1	*PR1*	Pathogenesis-related protein-1-like
FvH4_3g05950.1	*PR4*	Pathogenesis-related protein PR-4-like
FvH4_6g16950.1	*PR5.3*	Thaumatin-like protein
FvH4_3g28390.1	*BG2-1*	Glucan-endo-1,3-beta-glucosidase-like
FvH4_4g19500.1	B*G2-3*	Glucan-endo-1,3-beta-glucosidase, basic vacuolar is oform
FvH4_6g22790.1	*PGIP1*	Polygalacturonase-inhibiting protein
FvH4_4g05760.1	*PecLy1*	Probable pectate lyase 8
A. thaliana- MYB46-related genes		
At4g22680	*MYB85*	MYB transcription factor
At1g62990	*KNAT7*	KNOTTED-LIKE HOMEOBOX OF ARABIDOPSIS THALIANA 7
At5g44030	*CESA4*	Cellulose synthase A catalytic subunit 4
AT5g17420	*CESA7*	Cellulose synthase A catalytic subunit 7

AT4g18780	*CESA8*	Cellulose synthase A catalytic subunit 8

4.4.2 BLAST identification and primer design of potential direct targets of *FvMYB46*

To quantify putative transcripts coding for direct targets of primers were designed for qPCR. Although some of the primers seemed to work after testing on genomic DNA, qPCR resulted in these targets not being analyzed further. However, homolog identification and primer design is an important part of studying gene functions between species, and significant time went into this during my thesis work; thus, illustrations of the procedure were chosen to be presented as part of the results. The genes in the *MYB46*-pathway from *A. thaliana* that were chosen for this study were used for BLAST identification of homologous proteins in *F. vesca*. The *A. thaliana* proteins were identified using the gene ID (table 4.4.2).

Table 4.4.3: *Genes related to MYB46 in A. thaliana that were chosen for closer studies in this experiment. The reference denotes article(s) describing the gene or its link to MYB46. The potential homologous proteins in F. vesca were predicted in BLAST; the accession number for the corresponding mRNA is given in parenthesis. The sequence identity match and query cover are given in percentile values. For MYB85, two proteins were selected due to the second one also being of sufficient identity match. For the remaining genes, one single protein sequence was selected. References explaining the A. thaliana gene's relation to AtMYB46 are provided.*

At gene	Reference	Fv potential homologous protein	% identity match	% Query cover
MYB85	(Zhong et al., 2007)	ODORANT1 (XM_004298631.2)	90.91	13.0
		ODORANT 1-like (XM_004307779.2)	88.64	13.0
KNAT7	(Zhong et al., 2007)	Homeobox protein -knotted 1-like 7 (XM_004298679)	82.46	90
CESA4	(Ramirez et al., 2011b)	Cellulose synthase A catalytic subunit 4 (XM_004289933.2)	98.0	81.26
CESA7	(Ramirez et al., 2011b)	Cellulose synthase A catalytic subunit 7 (XM_004287096.2)	100.0	85.17
CESA8	(Ramirez et al., 2011b)	Cellulose synthase A catalytic subunit 8 XM_011462320.1	99.0	79.43

Primer pair 6

	Sequence (5'->3')	Template strand	Length	Start	Stop	Tm	GC%	Self complementarity	Self 3' complementarity
Forward primer	AAATGGCCAGTGTTGCTGGA	Plus	20	270	289	60.47	50.00	6.00	1.00
Reverse primer	TCTCTTCAAGTCGGGACGGA	Minus	20	378	359	60.25	55.00	5.00	2.00
Product length	109								

Products on intended targets

>XM_004298631.2 PREDICTED: Fragaria vesca subsp. vesca protein ODORANT1 (LOC101295622), mRNA

```
product length = 109
Forward primer  1    AAATGGCCAGTGTTGCTGGA  20
Template        270  ....................  289

Reverse primer  1    TCTCTTCAAGTCGGGACGGA  20
Template        378  ....................  359
```

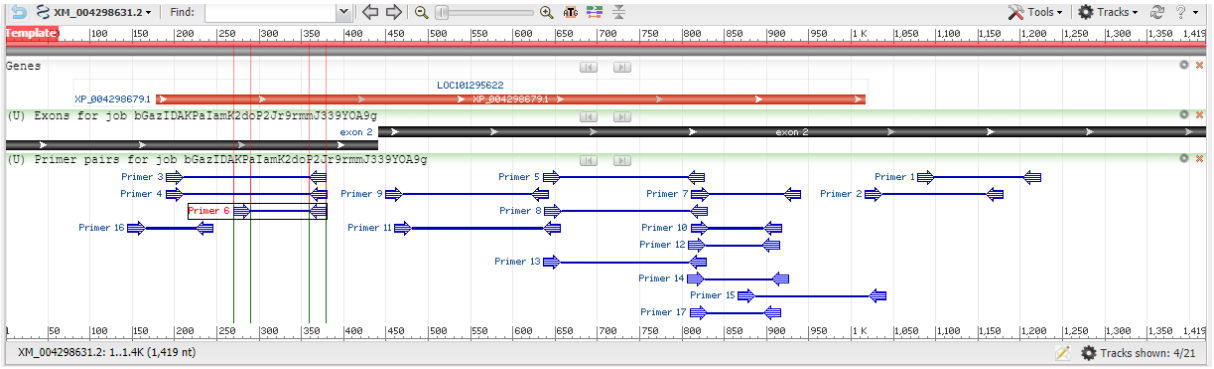

Fig 4.4.3: *example screenshot from the 'Pick Primers' function in NCBI, when picking primers within the same exon for the mRNA of ODORANT-1. The traits of the primers are given in the top half of the figure. The bottom half shows the reference mRNA sequence of the gene.*

The primers of putative downstream targets of *FvMYB46* (table 4.4.3) were tested on genomic DNA of *F. vesca* using PCR/gel-electrophoresis, to test that they were working. Only two primer pairs out of the 12 ones designed actually seemed to work on genomic DNA. Another primer pair (KNAT7(2)) bound unspecifically, showing a product longer than the expected product size (fig 4.4.4).

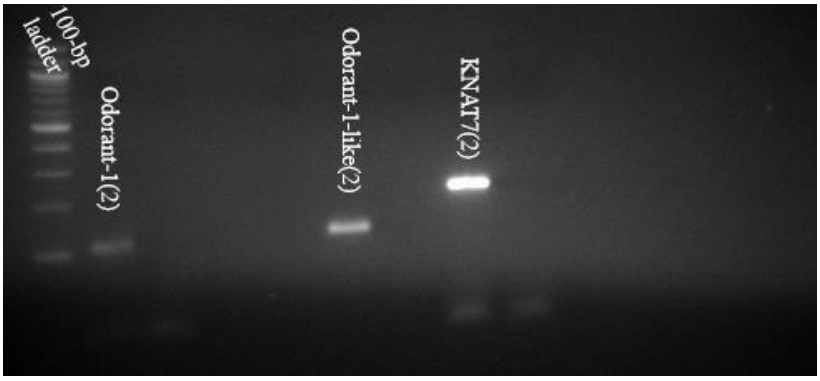

Figure 4.4.4: *Gel showing the binding of the designed primers to genomic DNA of F. vesca. Only primers Odorant-1(2) and Odorant-1-like(2) showed products of the expected sizes (109 and 144 bp, respectively). KNAT7(2) bound to an unspecific region, as the expected product of this primer was 140 bp and the product showed a band size of approximately 250 bp.*

4.5 Microscopy analyses of secondary cell walls

Microscopy analyses of *myb46* and WT flower stems were carried out to see differences in lignin content, both with and without inoculation using *B. cinerea*. Floral proximal stem sections of T0 plants at 48 hours post inoculation with *B. cinerea*: 4 B-plants and 4 *myb46*-plants where 2 of each were mock-inoculated, were investigated by light microscopy and fluorescence, with and without staining with Safranine O (fig 4.5.1) or IKI (fig 4.5.4). IKI, which stains starch granules, was chosen to properly distinguish starch from other tissue. Safranine O was used for staining of lignin-rich tissue. The main objective of these analyses were to see whether there were any visible differences in lignin content in B- and *myb46*-plants, as observed for *A.* thaliana in (Ramirez et al., 2011a).

Normal observations with conventional bright field microscopy did not indicate any expected differences between the mutant and WT (fig 4.5.1 A-H). Under UV lighting, however, there seemed to be a difference in autofluorescence in the endodermal region (fig 4.5.1 M and O). B-plants with *MYB46* intact showed higher autofluorescence than the *myb46* plants, with and without inoculation with *B. cinerea* (fig 4.5.1). Staining with safranine O also showed higher autofluorescence in the control plants compared to *myb46* mutants (fig 4.5.1 Q-X). These results could indicate that *myb46* mutants exhibit lower lignin deposition upon infection, although it should be noted that the amount of replicates was low.

At first glance, granules were thought to possibly be conidia of *B. cinerea*; this is why IKI was used. IKI staining indicated accumulation of starch grains in the endodermis of the observed sections (fig 4.5.4), and the impression that conidia may have accumulated in parenchymatous cells was disregarded.

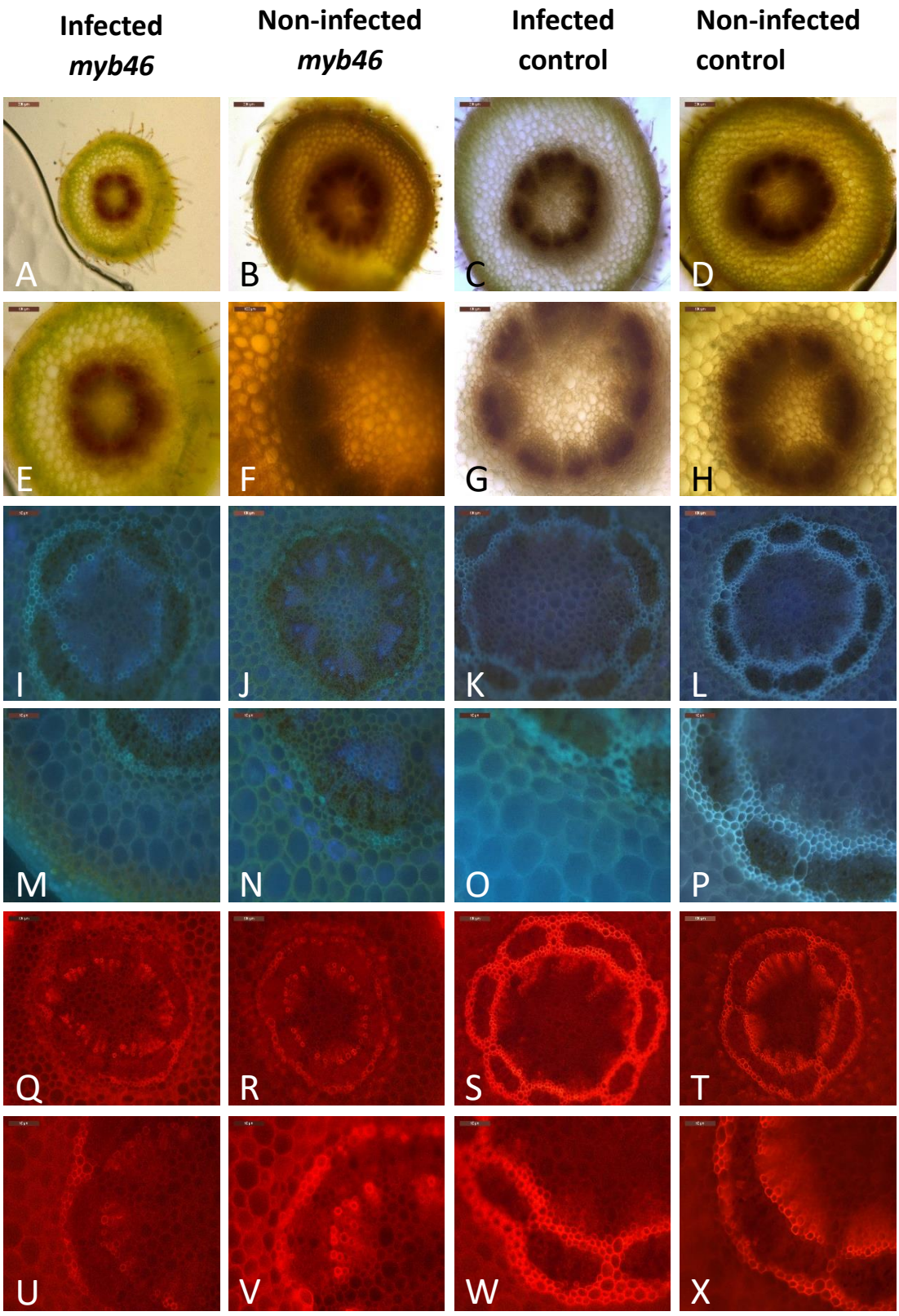

Figure 4.5.1: *Microscopal images of floral stem sections of F. vesca, fixated 48h after inoculation. Columns from left to right: inoculated myb46, mock-inoculated myb46, inoculated B-plant (control), and mock inoculated B-plant (control). Top two rows (A-H) show images taken with bright field microscopy, at 2 magnifications. Blue images (I-P) show images taken with fluorescence through a UV filter. Lignin autofluoresces as bright blue. Red images (Q-X) show images taken with fluorescence after staining with safranine O. The scales are as follows: 200 µm in row 1, 3 and 5; 100 µm in row 2, 4 and 6.*

To properly distinguish the different tissue observed by microscopy, figures were made with the assumed anatomical composition of the floral stem sections (fig 4.5.2 and 4.5.3). Furthermore, fig 4.5.4 illustrates the effect of IKI staining on starch visualization.

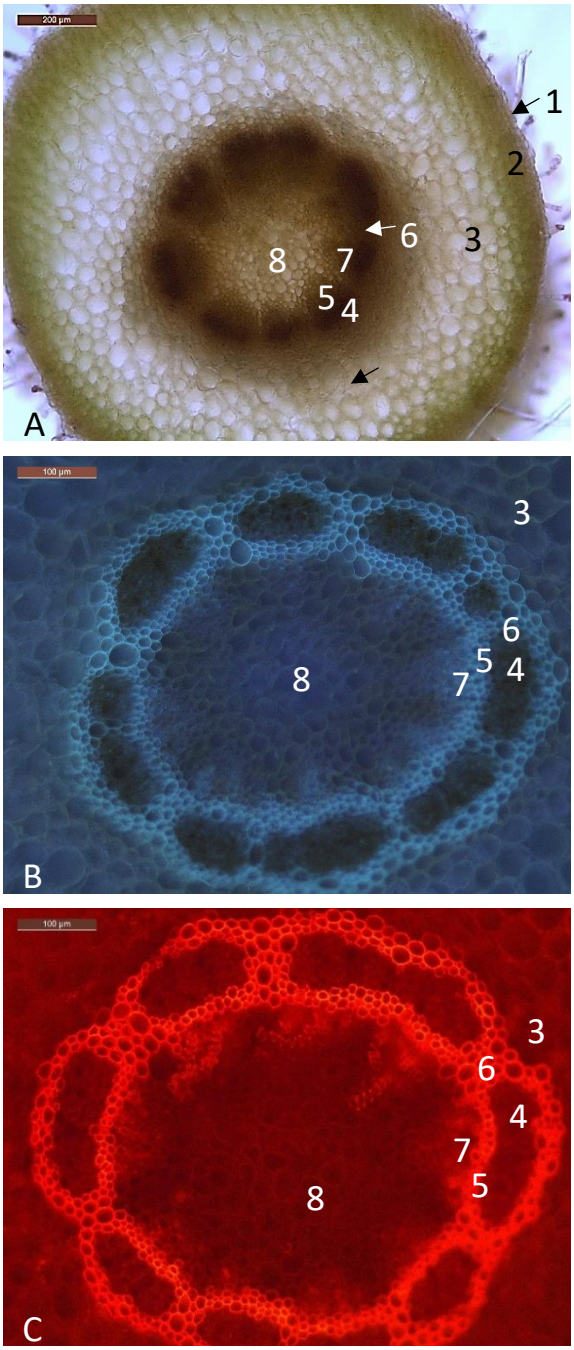

Figure 4.5.2: *Anatomy of strawberry flower stem. A. Overview of the entire stem. B. Overview of part of the stem with UV-filter. C. Overview of part of the stem with safranin fluorescence. Numbers indicate the different parts of the stem, as follows: 1. epidermis with trichomes; 2. cortex; 3. parenchyma; 4. phloem; 5. fascicular cambium; 6. interfascicular cambium; 7. xylem; 8. pith*

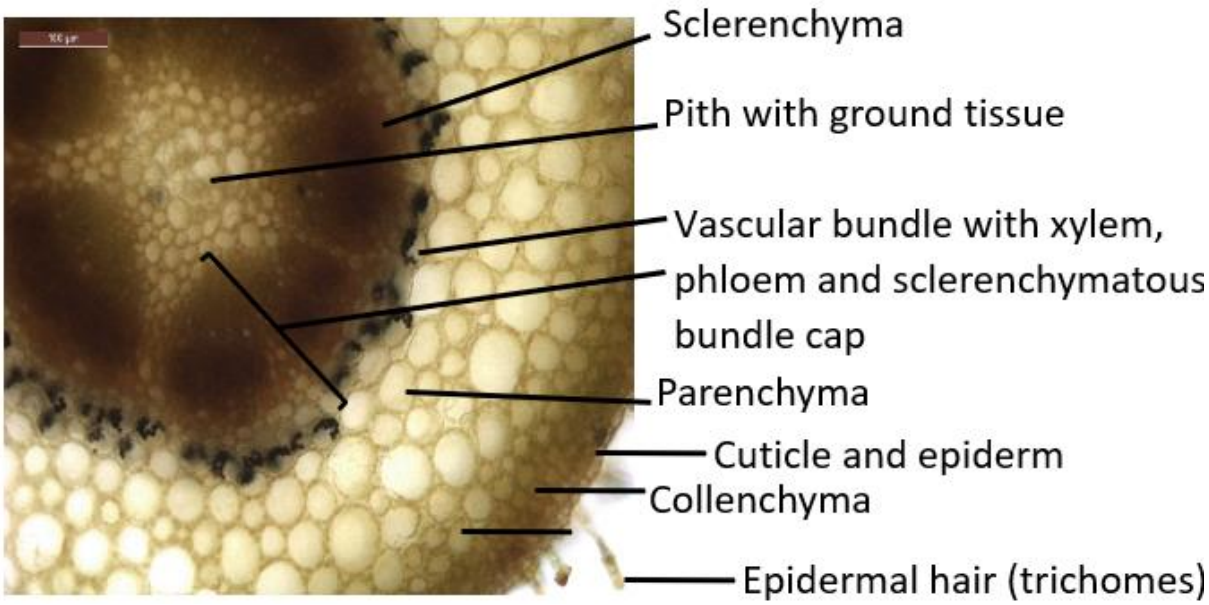

Fig 4.5.3: *illustration showing the assumed anatomy of the investigated stem sections.*

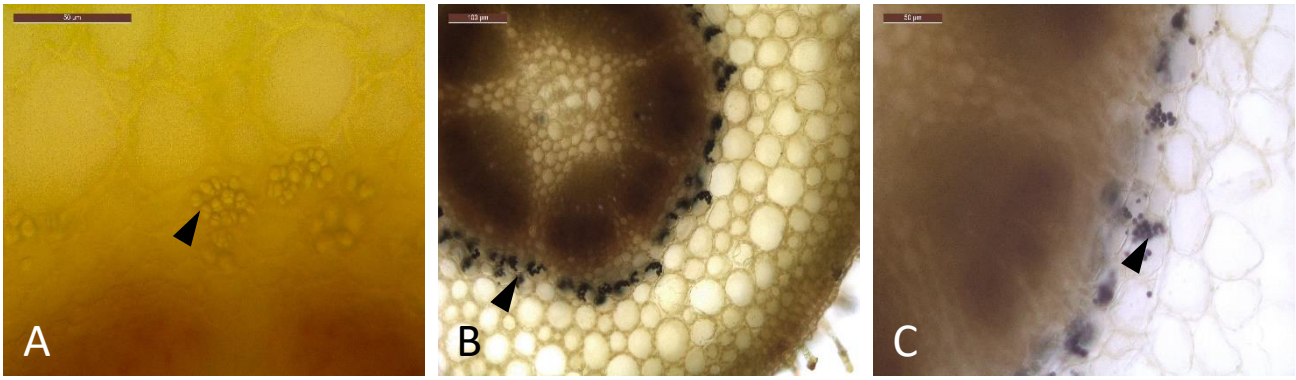

Fig 4.5.4: *bright field microscopy images showing the effect of IKI staining of F. vesca sections. A: unstained section with 50µm scale, B: stained section with 100µm scale, C: stained section with 50µm scale. Starch granules are visible without staining, however they are easier visualized with IKI staining, and confirmed not to be conidia of B. cinerea. Staining shows accumulation of starch near endodermis.*

4.6 Drought stress of detached leaves:

To see whether tolerance to osmotic stress was different between *myb46* mutants and WT-H4, detached leaf assays in different concentrations of mannitol (0, 150 and 300 mM) were carried out. mannitol is a polyhydric alcohol which can be used to incuce osmotic drought stress in plants (Możdżeń et al., 2015). Replicates of 3 leaflets for each of the genotypes WT, 43_T1

and 44_T1 (the two latter confirmed for *myb46* knock-out and without Cas9) were used for each treatment.

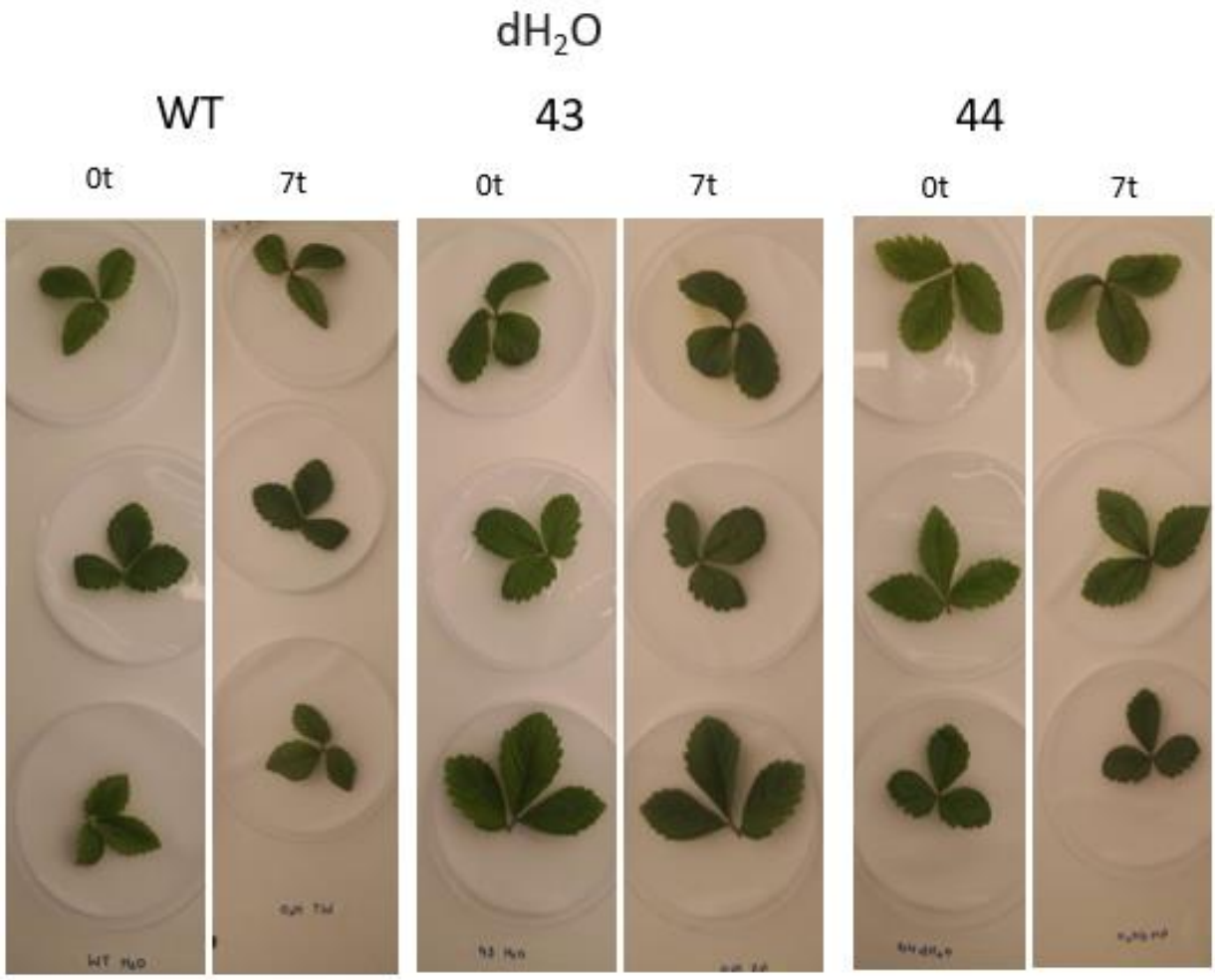

Fig 4.6.1: *Phenotypic development of leaves of WT and myb46(without Cas9) leaves placed on filter paper with dH_2O, photographed at 0 (0t) and 7 (7t) days after incubation.*

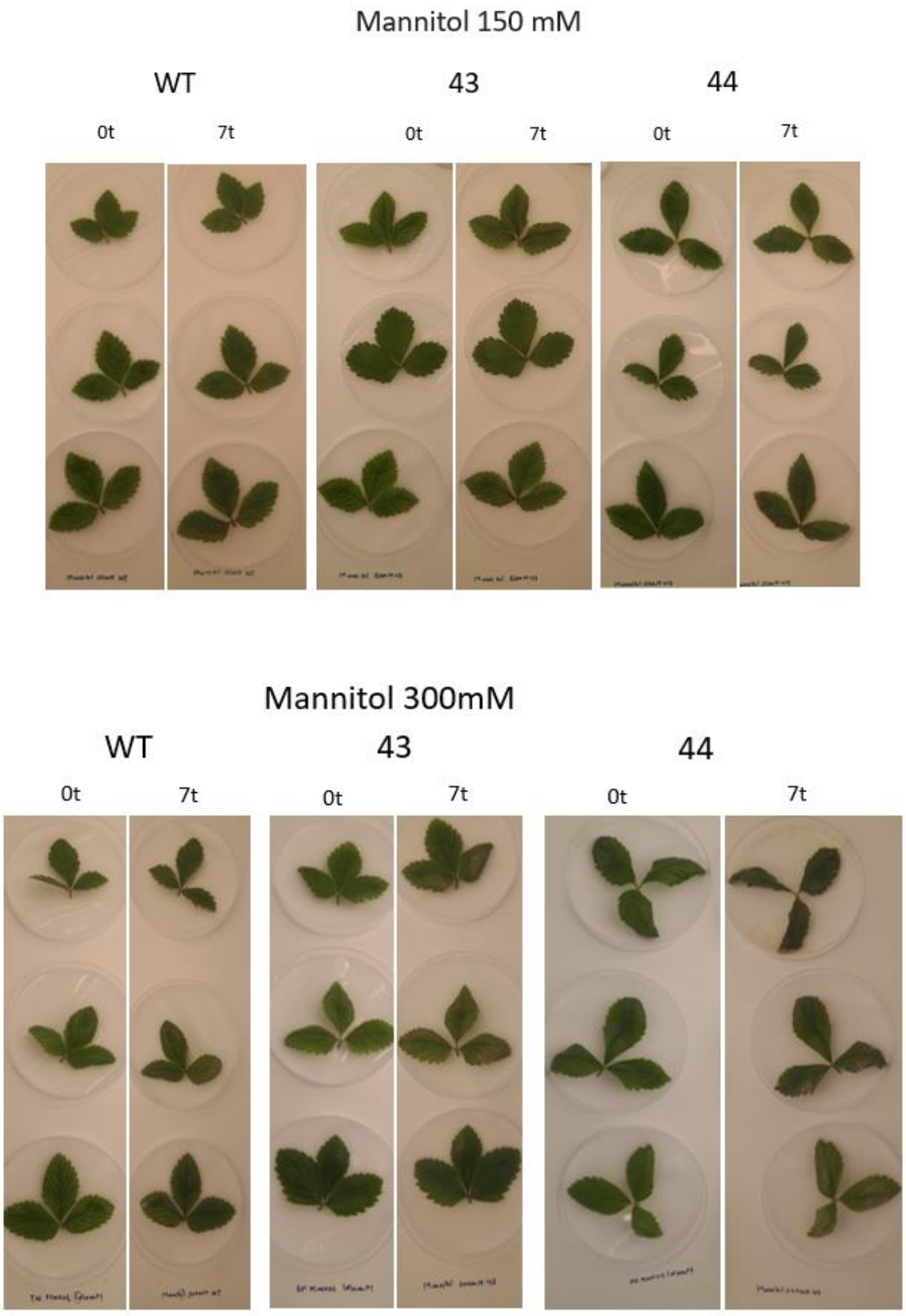

Fig 4.6.2 a) and b): *Phenotypic development of leaves of WT and myb46(without Cas9) leaves placed on filter paper with a) 150 mM and b) 300 mM mannitol at 0 (0t) and 7 days after incubation.*

Drought stress analyses of leaves showed little to no change in incubation with dH_2O after 7 days. In the 150 mM mannitol – containing samples (fig 4.6.2 a)), some changes in the leaves was observed. In the 300 mM mannitol – containing samples (fig 4.6.2 b)), some striking effects were seen after 7 days. Some of the leaves from *myb46* mutants (43 and 44) developed white-yellow spots on the leaf surface. This was not as prevalent in the WT – plants, indicating that there may be a difference in reacting to osmotic stress in *myb46* plants compared to WT. However, the sample size for this experiment was relatively low.

5 Discussion

5.1 Internal control plants displayed different phenotype during growth

In this thesis, the main objective was to investigate whether *Fvmyb46* mutants were more resistant to *B. cinerea*. Additionally, a number of experiments regarding the plants' phenotypes were conducted. During growth, the plants were observed for obvious phenotypic differences. The 3 B-plants/internal controls were used as controls for experiments conducted on the T0 generation. They were chosen as controls due to unavailable WT plants to grow along with the T0 primary transformants. Additionally, they were used as controls due to them having no deletion in *MYB46* but being positive for a truncated T-DNA insert (Magne Skårn, NIBIO), and thus could be used as independent transformants; however, it is likely that all three B-plants are clones due to identical phenotypes during growth. The B-plants showed a morphological phenotype different from that of *myb46* (fig 4.1.1). Since Cas9 surely was not present in the B-plants (fig 4.2.3), the truncated T-DNA(s) is likely causative of the observed phenotype. The insertion of the T-DNA(s) could have caused a mutation, either a bandshift -or missense mutation, or have led to an overexpression. Since we do know that the T-DNA is present, it is possible that another gene was overexpressed due to proximity to the 35S-promoter. T-DNAs contributing to overexpression of bordering genes has been observed (Halliday et al., 1999; Li et al., 2010) Sequencing these B-plants to find the site of the T-DNA and thus cause of their phenotype(s) could provide more insight into functional genomics of *F. vesca*.

All B-plants of T0 and V1 clearly grew slower (T0: fig 4.1.1), and at times would develop leaf and inflorescence lesions before their *myb46* counterparts during growth. Initially being chosen as control plants due to their present T-DNA insert but lack of *myb46* deletion, there is a chance that their phenotypes could have clouded the results in this study; for some of the

experiments, WT plants were grown along with the T1 progenies (without T-DNA) to use as controls; this would likely have proved to be the best basis for these experiments. The growth phenotypes of the B-plants (fig 4.1.1) may have altered the plants' development and pathogenic response system, leading to a difference in susceptibility or gene expression upon infection by *B. cinerea*. Secondly, the observed early leaf necrosis during growth (section 4.1), which was more prevalent in B-plants, could have caused a *priming* effect, thus rendering the B-plants more resistant/tolerant to imminent stress. The concept of priming involves the enhanced capacity to mobilize infection-induced cellular defense responses after a treatment, (Conrath et al., 2002) such as a pathogenic attack or hormonal application (Aranega-Bou et al., 2014). I here conclude that one should consider the peculiar phenotypes of B-plants observed during growth (fig 4.1.1 and 4.1.2) in the experiments conducted with them.

5.2 Genotyping of T0, T1 and V1 indicated two T-DNAs inherited as genetically linked

Use of PCR-(Gel electrophoresis) proved useful for detecting differences between the genotypes in T0, T1 and V1(section 4.2). An 81 bp deletion in *myb46* was easily visualized in the gel pictures. While Cas9 was observed in all investigated primary transformants, and not observed in B-plants (fig 4.2.3), the localization and copy number of Cas9 required further study to investigate. Genotyping of T0 based on (Inverse PCR data, Magne Skårn) indicated the presence of two T-DNAs, one putatively being shorter than the other. To gain further knowledge on the length of the T-DNAs as well as off-targets effects of the T-DNA inserts, one could use techniques such as whole-genome sequencing as in (Park et al., 2017) or southern blotting. Southern-blotting was chosen not to be performed in this project due to it involving the use of radioactive probes (Tage Thorstensen, personal communication).

In the T1 generation, Cas9 was segregated away for a selection of the plants. The goal for the T1 plants was to generate plants without Cas9, with a deletion in *myb46.* The segregation data showed close to a 1:1 segregation, while the expected ratio was 3:1 (Cas9:-Cas9) assuming a single copy of Cas9, or linkage between multiple copies. The ratio of 3:1 was expected due to the Cas9 being hemizygous and the plants most likely self-pollinating. However, the deviation was not big enough to conclude that Cas9 does not segregate in a 3:1 ratio; moreover, it should be noted that only a small sample size was investigated.

One of the T1-plants, 43-16, did not show a deletion in *myb46*. It may simply be that a WT-seed has been accidentally dropped into the sowing trays where T1 plants of T0-43 were

sown; sowing was done at the same time for all T1 seeds, along with WT seeds. Since the deletion of *myb46* is homozygous, and that they were expected to self-pollinate, all progenies of *myb46* mutants were expected to carry this deletion. Under the unlikely circumstance that pollination from outside the growth locations would occur, this could explain the presence of one *MYB46* progeny.

For one of the T1 plants from *myb46*-primary transformants (#43_T1_19)(fig 4.2.5a), Cas9 was confirmed to be present. However, PCR-genotyping of the known localizations (4.2.6a, 4.2.7a) based on inverse PCR (Inverse PCR data, Magne Skårn) indicated that Cas9 was localized elsewhere in this specific plant's genome; on the other hand, this could have been a false positive.

The remaining T1 plants that were positive for Cas9 were positive for both the known junctions (fig 4.2.6, 4.2.7), meaning that both T-DNA's were inherited together. The two T-DNAs are located closely to each other (Inverse PCR data, Magne Skårn). It is highly likely that the loci at which the T-DNAs are placed are genetically linked due to close localization and the observed consistency of both T-DNAs (fig 4.2.6, 4.2.7). It is also likely that the copy number of Cas9 is only one, since the same two regions of Cas9 were observed when they were positive for Cas9.

Although unlikely, the T-DNAs, depending on their localization, may have been causative for increased seed and/ or seedling lethality. If the T-DNA indeed cause a missense- or nonsense mutation leading to increased lethality, this could explain the skewed distribution of Cas9:-Cas9 plants in the T1 generation. An extreme example of T-DNA insertion effects is in (Zhou et al., 2014), where a hemizygous T-DNA insertion in AtTAD2- and AtTAD3- encoding genes led to complete lethality in *A. thaliana*, due to a loss of function of these important genes. Future knowledge about the effects of the T-DNAs in the specific insertion sites would be intriguing. Germination rates, as well as seedling survival rates for the seeds of the primary transformants (T0) were not assessed. Calculating germination rates for seeds of *myb46* mutants compared to WT could provide further knowledge on possible effects of 1) a deletion in *MYB46*, and 2) T-DNA inserts.

5.3 Detached tissue assays show no differences in susceptibility to grey mould

5.3.1 Detached leaf assays

Detached leaf assays to determine susceptibility to grey mould did not show the hypothesized significant results based on similarity to *MYB46* in *A. thaliana* (Ramirez et al., 2011a), that a

deletion in *FvMYB46* renders *F. vesca* less susceptible to *B. cinerea* (fig 4.3.3) compared to WT. The results however showed high variability in lesion sizes. This could be caused by a number of factors: a small data set, insufficiently optimized detached leaf assays, human mistakes during inoculation or preparation, induced resistance, or simply greatly varying susceptibility profiles between the leaves and plants. There is also a possibility that leaf age of selected leaves was uneven; in *F.* X *ananassa,* leaf susceptibility to *B. cinerea* decreases from 1 to 4 weeks of age, and increases after 5 weeks of age (Meng et al., 2019).

Puncturing of leaves was done manually using a pipette tip and puncturing in a slightly circular motion, likely to cause variable wound sizes and depths. Mechanical damage facilitates a point of entry for pathogens (Quilliam et al., 2006). Conversely, wounding can stimulate induced resistance in plants; in fact, this has been observed for resistance to *B. cinerea* in *A. thaliana* (Conrath, 2009). Variable wounding may thus have affected the lesion development variably in the observed leaves.

A detached leaf assay provides a rapid and non-destructive method of studying susceptibility in leaves. However, alternative methods to quantify how well a pathogen succeeds in infecting and spreading throughout a leaf exist. In a study by (Fister et al., 2018) where leaves of cocoa (*Theobroma cacao*) were inoculated with *Phytophthora tropicalis*, the presence of the pathogen was quantified using qPCR on isolated DNA at different time points. (Degani & Cernica, 2014) simply did qualitative measurements of disease development of *Harpophora maydis* in maize (*Zea mays* L.), as their results were distinguishable by visual observation. (Ramirez et al., 2011a) used Tryptan blue staining of leaves to detect the spread of fungal mycelia of different genotypes of *A. thaliana* in addition to measuring leaf lesion areas. Different methods for analyzing a detached leaf assay exist, and optimization of the analyses are required for the specific host and pathogen.

The detached leaf assays carried out in this experiment lead to the conclusion that *MYB46* does not *majorly* affect leaf resistance to *B. cinerea* in *F. vesca*. However, it is still possible that a percentile difference can be observed with more data.

For infection assays in general, detached tissue assays are often preferrable as they are non-destructive, require small incubation spaces and the climatic conditions are easy to control (Aregbesola et al., 2019). Conversely, whole-plant infection assays can possibly better emulate how a plant in more realistic conditions reacts to a pathogenic intrusion. (Liu et al., 2007) found vastly different defense responses between attached and detached leaves of *A.*

thaliana inoculated with *Colletotrichum* isolates. Interestingly, in their study, pathogenesis-related gene *PR1* expression was associated with the salicylic acid- and ethylene-dependent pathways when attached, and provided increased resistance compared to the detached leaves; the detached leaves on the other hand were more susceptible and were decoupled to these hormonal defense pathways (Liu et al., 2007). There is also reason to suspect that the jasmonic acid-pathway may be affected in detaching a leaf from the rest of the plants; jasmonic acid is transmitted through vascular bundles as long-distance signals (Ruan et al., 2019), which may be important for defense responses in attached leaves. Supplementary whole-plant infection assays could provide different resistance exhibition between the genotypes as well as more insight into the defense-related pathways affected by *MYB46*.

5.3.2 Detached flower assays

The detached flower assays did not show any indication that inflorescence resistance to *B. cinerea* is affected by this specific deletion in *MYB46* (fig 4.3.4, 4.3.5) . Similar disease development was observed between plants of *myb46* and the internal controls. Detached flower assays were carried out to see whether *MYB46* affected flower susceptibility to *B. cinerea*. Grey mould is normally a problem in fruits and flowers of strawberries (Petrasch et al., 2019); therefore, investigating the disease effects on flowers may be more important than on leaves. Additionally, *MYB46* has been found to be more expressed in flowers than in leaves of *A. thaliana* (Zhong et al., 2007).

The arbitrary disease severity ranking from 0 to 4 (Darras et al., 2006) used in this study does not utilize specific lesion and infection sizes. The measurement system provides a number based on estimated lesion area of the petals. This scoring system is thus less applicable for finding small percentile differences in susceptibility, however it can provide a rapid indication of the disease severity in greater datasets. For identification of small differences in susceptibility, a more thorough approach would be required such as measuring relative lesion measurements. Still, the detached flower assay in this study provides a good indication that the specific *MYB46* deletion does not majorly affect flower disease development of *B. cinerea* in *F. vesca*.

It is possible that other means to inoculate than drop inoculation of conidial suspension could have given more reliable results. Drop inoculation in three spots facilitates pathogenic establishment in the spots of the droplets, however the petals not covered by drops are only affected when the pathogen eventually spreads to these petals. A spray inoculation method,

such as the one done by (Donati et al., 2018) could have facilitated a more even distribution of conidial suspension.

As inflorescences are the predecessors to berries, studying their disease development may provide more economically relevant findings for researchers and farmers, both pre- and postharvest. The detached flower assay could also be an important tool to study postharvest disease development. For this study, learning more about expression of *MYB46* in inflorescence and berry tissue could be useful from an agroeconomical standpoint.

5.3.3 Lack of difference in detached tissue assays could be explained by species-specific functions of *MYB46*

What could be the cause of *MYB46* acting as a susceptibility gene to *B. cinerea* in *A. thaliana*, but not in *F. vesca*? Firstly, since *AtMYB46* acts redundantly with *AtMYB83* (McCarthy et al., 2009), it is possible that a *F. vesca* -homolog of *MYB83* compensates for the truncated transcript of *FvMYB46*. Secondly, the function of *MYB46* seems to predominantly affect secondary cell wall composition in other species than *A. thaliana*, such as rice (*Oryza sativa*)(Zhong et al., 2011), apple (*M. domestica)*(Chen et al., 2019) and birch (*B. platyphylla*)(Guo et al., 2017). The resistance inducing phenotype caused by *MYB46* in *A. thaliana* (Ramirez et al., 2011a) may be species specific; at the time of writing, there are no published papers describing *MYB46* affecting resistance to *B. cinerea* in other species than *A. thaliana.* Thirdly, there could simply be that *myb46* knock-outs generated did not affect *MYB46* expression and/or translation, that a larger knock-out, or a knock-out in a different region would have generated more distinct phenotypes.

The specific deletion in *FvMYB46* may not have affected resistance responses at all. Using BLAST searches with the *A. thaliana MYB46* reveals two highly similar candidate genes in *F. vesca*. Only a deletion in the first of these two was generated in this study. It is thus possible that deleting the second of these genes would have caused different phenotypes than seen here, and that the "wrong" gene was knocked out. (Tage Thorstensen, personal communication)

The edible part, the berry, of strawberry is the most economically important. *B. cinerea* affects berries both pre- and postharvest. In a study like this, it is imperative to investigate or contribute to predicting the effects on berries in addition to leaves and flowers. In this study, no experiments with berries were carried out, due to low amounts of viable berries appearing in the same growth stage at the same time points. Additionally, very few berries of the control plants reached sufficient ripening. A separate detached fruit assay as a separate experiment

could have been performed if there had been material to do so. A detached fruit assay could provide more insight to the economically impactious traits of *myb46* mutants. Moreover, *MYB46* could affect other traits such as yield and fruit quality, however this remains to be investigated.

5.4 Expression of *PR4, PR5.3* and *BG2-3* is lower in inoculated *myb46* mutants

The qPCR performed on inoculated and non-treated leaves of *myb46* and B-plants (fig 4.4.2) showed some varying results. It was expected that a handful of pathogenesis-related genes would be upregulated upon infection, and that *myb46* plants would have higher expression of these genes compared to the B-plants, as a consequence of hypothesized higher resistance; however, differences in susceptibility were not observed in detached leaf or detached flower assays.

Based on (Badmi et al., 2019), *BG2-3*, *PR4*, *PR5.3* and *PGIP1* were all expected to be upregulated upon infection with *B. cinerea*. *PR4* seems to be highly upregulated in both *myb46* and B-plants in inoculated leaves compared to untreated leaves (myb-base and b-base)(fig 4.4.2b). *PR4* was relatively higher expressed in infected B-plants compared to infected *myb46*-plants. *PR4* encodes a fungal chitin-inhibitory protein (Bertini et al., 2012). It is possible that this gene is less activated in *Fvmyb46* mutants than in internal controls.

PR5.3 was highly upregulated in untreated B-plants. In fact, higher than for inoculated B-plants; conversely, *myb46* leaves showed higher expression of *PR5.3* when inoculated compared to non-treated leaves of *myb46* (fig 4.4.2c). *PR5.3* is a homolog of a thaumatin-like protein, *PR5*, which is involved in pathogenic response, but has been linked to a number of abiotic and biotic factors in different plant species (de Jesus-Pires et al., 2020) It is possible that one of the non-treated B-plants, which showed a very high value for expression of *PR5.3* was highly upregulated in untreated B-plants by another stress factor, such as drought, prior to harvest.

PGIP1 was upregulated in infected plants, with similar expression levels between infected plants of *myb46* and internal controls. *PGIP1* is an important inhibitor of fungal polygalacturonase, and has been linked positively with resistance to *B. cinerea* (AbuQamar et al., 2017). *BG2-3* exhibited greatly increased expression after inoculation with *B. cinerea*, both in *myb46* mutants and B-plants, however this was more pronounced in B-plants. *BG2-3*

is an homolog of an *A. thaliana* ß-1.3-glucanase, which is implicated to be involved in plant defense (Uknes et al., 1992).

Both *PR1* and *PecLy1* were expected to be downregulated after infection with *B. cinerea*, based on (Badmi et al., 2019). *PR1* was also seemingly reduced, as the untreated ('base') leaves showed some expression of *PR1*, while the inoculated leaves did not (fig 4.4.1a). In *A. thaliana*, *PR1* expression is induced upon infection with *B. cinerea* (Ferrari et al., 2007); however, (Badmi et al., 2019) observed the opposite, that expression of the *F. vesca* homolog *PR1* is reduced after infection. A reduction in *PR1* is compliant with the observed values of Badmi and colleagues.

Expression of *PecLy1* was reduced after pathogenic insult with *B. cinerea*, as expected based on (Badmi et al., 2019). Expression was similar in untreated B-plants and *myb46* mutants, however much more variable in B-plants (fig 4.4.1f). *PecLy1* is a homolog of Probable pectate lyase 8 from *A. thaliana*, a protein involved in the breakdown of pectin (Uniprot, 2000). It is possible that the reduced expression upon infection is a result of a change in the pectin-breakdown pathway.

5.4.1 *MYB46* deletion may not affect expression of *MYB46*

MYB46 was expressed in low amounts (fig 4.4.1) in all treatments. Surprisingly, in *myb46* mutants, *MYB46* was seemingly, although insignificantly, higher expressed than the B-plants. This suggests that the *myb46* deletion itself might not result in lower *MYB46* expression; qPCR-primers for *MYB46* were localized outside of the deleted area, and thus may not be affected by a missing part of the same gene. Investigating the length of these transcripts could be interesting, to see whether transcripts or proteins are truncated as a consequence of the deletion. *MYB46* was less expressed in B-plants inoculated with *B. cinerea* compared to the non-treated B-plants, while being more expressed in inoculated *myb46* plants compared to untreated *myb46* plants. Since the results are variable, it is difficult to conclude the effect of a deletion in *MYB46* on expression of *MYB46* in *F. vesca*. (Ramirez et al., 2011a) found unchanged levels of *MYB46* between Col-0 plants with and without pathogenic infection, however, one of their *Atmyb46* deletion lines generated significantly lower expression of *AtMYB46* without pathogenic infection compared to Col-0. Expression of *MYB46* may be unaffected in this study, however studying the size and function of the transcripts could be of future interest.

5.4.2 A few sources of error may have caused high variability in expression

Some of the qPCR results were quite variable, with large standard errors (fig 4.4.1a-d, f). qPCR requires careful handling and accuracy throughout the procedure, and as such there are many potential human sources of error. Additionally, as only two or three biological replicates were used for expression analyses, it is likely that increasing the amount of replicates would reduce the standard deviation of the analyses. (Badmi et al., 2019) used a relative expression value based on quantification of *B. cinerea* DNA in the sample, and corrected the Ct value of pathogenesis-related genes, thus linking expression levels directly with the amount of *B. cinerea*; in this study, the same could be done here to account for the relative presence of pathogens. Furthermore the incubation time (48 h) may have affected the leaves differently. Some leaves developed slight lesions after 48 hours, as seen in chapter 4.3, while others did not, suggesting that lesion development for most leaves starts somewhere between 2 and 5 dpi. It would have been better to harvest RNA already after 24 hpi, as in (Badmi et al., 2019). Pathogenesis-related genes may already be affected greatly at 24 hpi, while seeing a reduction at times after this, due to the accumulation of secondary metabolites (Jacobo-Velazquez et al., 2015), for example, in apple (*M. domestica*), expression of chitinases is high after 12 hours, while being dramatically reduced after 48 hours (Tian et al., 2019).

5.4.3 A few defense-related are lower expressed in *MYB46*

Although the expression analyses of *myb46* and B-plants showed variable results, some conclusions can be drawn. Expression of *PR4* (fig 4.4.1b) and *PR5.3* (fig 4.4.1c) was significantly lower in inoculated *myb46* mutants compared to inoculated B-plants; however, for *PR5.3*, untreated B-plants exhibited high expression as well. Additionally, *BG2-3* (fig 4.4.1e) was less expressed in inoculated *myb46* mutants compared to inoculated B-plants, however this difference was not significant. It was expected that these genes would be upregulated in more resistant plants as upregulated defense responses based on (Badmi et al., 2019). Although not proved phenotypically, the results from expression analyses could indicate that defense responses in *myb46* plants are less activated than in B-plants. However, as a consequence of variability and, possibly, too long incubation times, further study is required.

5.5 Microscopy shows lower lignin accumulation in *myb46* mutants than B-plants:

The microscopy assays of flower stem sections provided some interesting results. Autofluorescent signals under UV -lighting (fig 4.5.1 I-P), as well as under intensified green fluorescent light after staining with Safranine O (fig 4.5.1 Q-X) showed lignin accumulation

in sclerenchymal interfascicular cells of B-plants both with an without inoculation; conversely, stem sections of *myb46*-mutants did not show lignin accumulation as for B-plants (fig. 4.5.1). This leads to the indication that lignin deposition in secondary cell walls of flower stems of *F. vesca* is lower in *myb46*-mutants than in B-plants, regardless of being inoculated or not; similar findings have been found in *MYB46* in apple (Chen et al., 2019) and birch (Guo et al., 2017). Furthermore, microscopy results in (Ramirez et al., 2011a) indicated lower lignin deposition in *Atmyb46* mutants than Col-0, and conversely higher lignin deposition in *MYB46*-overexpressed lines. There is thus compliance in the microscopy results here on the function of *MYB46* in other species.

Based on the findings through microscopy and staining, I hypothesize that the transcriptional network of *F.vesca MYB46* positively regulates lignification of cell walls of interfascicular cells of floral stems, as in (Ramirez et al., 2011a). I was only able to utilize primers for a few homologous downstream putative targets of *AtMYB46* in *F. vesca*; moreover, expression analysis did not show any detection of transcripts, resulting in discardment from the results. (Zhong et al., 2007) found that *AtMYB46* predominantly is expressed in inflorescence stems, which may explain the low expression of *FvMYB46* (fig 4.4.2) in my leaf data. Attempts were made to make expression analyses for flowers, however low amounts of flowers from B-plants were available at each time of assessment. The transcriptional regulatory network of *FvMYB46* thus still requires more study. For the future, expression studies on the *FvMYB46* regulatory pathway in flowers rather than leaves should provide findings explaining the differences in flower stem lignin deposition.

5.5.1 The lignin biosynthesis pathway could be affected by cellulose synthases

How can lignin biostynthesis be upregulated by expression of *MYB46*? Lignin is a biopolymer found abundantly in xylem cells, which in turn are composed of dead cells functioning to provide structural support and facilitate water transport throughout the plants. Development of lignified cells occurs upon a variety of processes; during cell morphogenesis, secondary cell wall deposition and programmed cell death (Smith et al., 2013). It is most likely that the observed lignin differences are a consequence of secondary cell wall deposition. *MYB46* acts as a master switch of the secondary wall biosynthetic program in a number of species (e.g. rice, Arabidopsis, poplar and maize) (Kim et al., 2013), and regulates the expression of a number of genes, among which are *CESA4*, *CESA7* and *CESA8*, all secondary wall cellulose synthases. Upon increased expression of *AtMYB46*, the expression of *CESA4*, *CESA7* and *CESA8* is upregulated (Kim et al., 2013). As I was not able to find suitable primers for

expression analyses of downstream *MYB46* target homologs in this study, we do not know if a similar expression pattern can be seen in *F. vesca* upon altered transcription of *MYB46*. However, if lignin deposition indeed is proven to be downregulated in *Fvmyb46* mutants, *FvMYB46* must play a role in secondary wall biosynthesis.

Although not observed in this study, how can a deletion in *MYB46* and thus lignification of secondary cell walls be associated with increased pathogenic resistance? (Ramirez et al., 2011a) ties the function of *MYB46* as a susceptibility gene to the upregulation of Ep5C- a Type III Peroxidase originally identified in *Solanum lycopersicum* (tomato)- when *MYB46* expression is reduced, as shown in (Coego et al., 2005). Furthermore, (Ramirez et al., 2011a) showed that *myb46* mutants had higher Ep5c promoter activity following pathogenic inoculation. The upregulation of type III peroxidases can be linked to both cell wall repositioning, lignification, as well as controlling apoplastic and vacuolar functions (Veljović Jovanović et al., 2018). Moreover, this family of peroxidases contributes to production of reactive oxygen species, as well as peroxidases, both possible contributors to increased pathogenic defense.

Lignified cell walls can be regarded as a physical barrier to avirulent pathogens, effectively trapping and terminating the growth of pathogens. This renders plants resistant to a number of pathogens when the cell walls are intact; furthermore, motility of pathogens is negatively affected by lignin accumulation (Lee et al., 2019). It is as such possible that inoculation without mechanical wounding (as was done in detached flower assays) is less effective in plants with higher lignin contents, such as the B-plants compared to *Fvmyb46* mutants; lack of wounding would thus facilitate a more rapid breach of the physical barrier in *Fvmyb46*, since it contains less lignin. For improvement of this study, the detached flower assays should have been carried out with as well as without wounding, to see whether wounding changed the susceptibility between the B-plants and *myb46* mutants.

5.5.2 Future perspectives for increased validity of microscopy observations

Microscopy investigations indicated higher lignin deposition in internal controls compared to *myb46* mutants (fig 4.5.1). Although this was visually observed, lignin contents were not measured quantitatively in this study. To further prove the observed lignin differences, further studies could revolve around measuring lignin contents in addition to other cell wall constituents. (Ramirez et al., 2011a) observed a slight increase in leaf lignin content in overexpressed lines of *AtMYB46* compared to Col-0 and *Atmyb46*, however no significant differences between Col-0 and *Atmyb46*. For novelty beyond this study, investigating the

lignin content as well as other cell wall constituents before and after pathogen inoculation in flowers (Cosio & Dunand, 2010) and leaves (Lee et al., 2019) could provide quantitative evidence of the differences observed by microscopy.

Some factors should be regarded when looking at the results for microscopy. Firstly, only two replicates were used for each treatment in the microscopy study. However, for both replicates, similar fluorescence profiles were observed. Although the results observed seem plausible based on theory, a bigger sample size would further substantiate the validity of the observations. Secondly, a light microscope was used instead of a confocal microscope. A confocal microscope allows for multidimensional modeling through profiles of a cell section (Elliott, 2020). Furthermore, stem sections were cut by hand, and may consequently have been of variable thickness. This may have caused variability in fluorescence between the investigated sections. To further increase the validity of the microscopy analyses, studies using a bigger dataset are required.

5.6 *FvMYB46* could be an important gene in regulating osmotic stress responses:

Phenotypic testing of detached leaves of *F. vesca* in different concentrations of mannitol provided some interesting results. It seemed, based on qualitative assessments (fig 4.6.1 and 4.6.2) that leaves of *myb46* mutants, especially leaves of #44_T1 (#44_T1_1, #44_T1_2, #44_T1_3, #44_T1_4), developed stronger symptoms of drought than leaves of WT. This could mean that *FvMYB46* acts as a transcription factor for genes related to osmotic stress. As seen in (Guo et al., 2017) and (Chen et al., 2019), *MYB46* overexpression in both birch and apple leads to increased osmotic stress tolerance; these studies also found upregulation of lignin-biosynthesis related genes and subsequently lignin content in overexpressed *MYB46* lines along with reduction in transpiration, as described in (section 5.6). In my study, no genes related to lignin biosynthesis or general stress responses were investigated. Moreover, only a small sample size was utilized (n= 3x3x3). By expanding the sample size as well as investigating the expression of genes related to stress, further experiments the osmotic stress effects of *myb46* could provide more elaboration on the potential stress-related mechanisms of *FvMYB46*.

6 Conclusion

The main objective of this thesis was to investigate the effects of CRISPR/Cas9-generated lines of *Fragaria vesca-myb46* knock-outs on susceptibility to *B. cinerea*; the hypothesis being that *MYB46* acts as a susceptibility gene to *B. cinerea*, thus rendering *myb46* knock-out plants more resistant. Additionally, lignin contents of floral stems as well as osmotic tolerance in these transgenic lines were investigated, to see other phenotypic effects of a deletion in *myb46* as seen for *MYB46*-homologs in other plants.

Detached tissue pathogenicity assays were carried out to study resistance differences in *myb46* plants compared to WT in detached leaf assays and compared to internal controls in detached flower assays. These results did not conclude any differences in *B. cinerea* susceptibility between *myb46* and the other genotypes. Additionally, expression analyses were carried out to see if defense responses were different between the two genotypes upon infection with infection of *B. cinerea*. Some of the results suggest that pathogenicity-related genes are lower expressed in *myb46* mutants, and that *MYB46* itself is more expressed although possibly a truncated version. Microscopy analyses and staining of proximal flower stems indicated more lignin content in our internal control plants compared to those of *myb46*. Thus, *MYB46* could play an important part in floral stem lignin deposition in *F. vesca*. Exposure of leaves of *F. vesca* to drought stress by use of mannitol indicated that *myb46* leaves may be more susceptible to adverse osmotic stress. It is as such possible that *FvMYB46* plays a role in gene regulation in response to drought stress.

Plant pathogens and drought are two important damaging factors that cause a number of challenges for farmers and the world food security as a whole. To combat the food security issues facing the world it is of paramount importance that we improve crops and agronomical practices. The emergence of gene editing techniques such as CRISPR/Cas9 allow for scientists to study the functions of genes such as *MYB46* to potentially develop more suitable crop varieties. Although some functions of *MYB46* in *F. vesca* have been investigated in this study, some of its characteristics are yet to be fully mapped. More extensive study on the relationship between *FvMYB46* and disease resistance, lignin and secondary cell wall deposition as well as osmotic stress are required.

7 References

AbuQamar, S., Moustafa, K. & Tran, L. S. (2017). Mechanisms and strategies of plant defense against Botrytis cinerea. *Crit Rev Biotechnol*, 37 (2): 262-274. doi: 10.1080/07388551.2016.1271767.

Agrios, G. N. (2005). *Plant Pathology*. 5 ed.: Dana Dreibelbis.

Albinsson, B., Li, S., Lundquist, K. & Stomberg, R. (1999). The origin of lignin fluorescence. *Journal of Molecular Structure*, 508 (1-3): 19-27. doi: 10.1016/s0022-2860(98)00913-2.

Ambawat, S., Sharma, P., Yadav, N. R. & Yadav, R. C. (2013). MYB transcription factor genes as regulators for plant responses: an overview. *Physiol Mol Biol Plants*, 19 (3): 307-21. doi: 10.1007/s12298-013-0179-1.

Amil-Ruiz, F., Blanco-Portales, R., Munoz-Blanco, J. & Caballero, J. L. (2011). The strawberry plant defense mechanism: a molecular review. *Plant Cell Physiol*, 52 (11): 1873-903. doi: 10.1093/pcp/pcr136.

Aranega-Bou, P., de la, O. L. M., Finiti, I., Garcia-Agustin, P. & Gonzalez-Bosch, C. (2014). Priming of plant resistance by natural compounds. Hexanoic acid as a model. *Front Plant Sci*, 5: 488. doi: 10.3389/fpls.2014.00488.

Aregbesola, E., Ortega-Beltran, A., Falade, T., Jonathan, G., Hearne, S. & Bandyopadhyay, R. (2019). A detached leaf assay to rapidly screen for resistance of maize to Bipolaris maydis, the causal agent of southern corn leaf blight. *European Journal of Plant Pathology*, 156 (1): 133-145. doi: 10.1007/s10658-019-01870-4.

Audenaert, K., De Meyer, G. B. & Hofte, M. M. (2002). Abscisic acid determines basal susceptibility of tomato to Botrytis cinerea and suppresses salicylic acid-dependent signaling mechanisms. *Plant Physiol*, 128 (2): 491-501. doi: 10.1104/pp.010605.

Babaeizad, V., Imani, J., Kogel, K. H., Eichmann, R. & Huckelhoven, R. (2009). Over-expression of the cell death regulator BAX inhibitor-1 in barley confers reduced or enhanced susceptibility to distinct fungal pathogens. *Theor Appl Genet*, 118 (3): 455-63. doi: 10.1007/s00122-008-0912-2.

Badmi, R., Zhang, Y., Tengs, T., Brurberg, M. B., Krokene, P., Fossdal, C. G., Hytönen, T. & Thorstensen, T. (2019). Induced and primed defense responses of Fragaria vesca to Botrytis cinerea

doi: 10.1101/692491.

Balint-Kurti, P. (2019). The plant hypersensitive response: concepts, control and consequences. *Mol Plant Pathol*, 20 (8): 1163-1178. doi: 10.1111/mpp.12821.

Belhaj, K., Chaparro-Garcia, A., Kamoun, S. & Nekrasov, V. (2013). Plant genome editing made easy: targeted mutagenesis in model and crop plants using the CRISPR/Cas system. *Plant Methods*, 9 (1): 39. doi: 10.1186/1746-4811-9-39.

Bertini, L., Proietti, S., Aleandri, M. P., Mondello, F., Sandini, S., Caporale, C. & Caruso, C. (2012). Modular structure of HEL protein from Arabidopsis reveals new potential functions for PR-4 proteins. *Biological Chemistry*, 393 (12): 1533-1546. doi: 10.1515/hsz-2012-0225.

Bestfleisch, M., Luderer-Pflimpfl, M., Höfer, M., Schulte, E., Wünsche, J. N., Hanke, M. V. & Flachowsky, H. (2015). Evaluation of strawberry (FragariaL.) genetic resources for resistance toBotrytis cinerea. *Plant Pathology*, 64 (2): 396-405. doi: 10.1111/ppa.12278.

Bond, J., Donaldson, L., Hill, S. & Hitchcock, K. (2008). Safranine fluorescent staining of wood cell walls. *Biotech Histochem*, 83 (3-4): 161-71. doi: 10.1080/10520290802373354.

Borrelli, V. M. G., Brambilla, V., Rogowsky, P., Marocco, A. & Lanubile, A. (2018). The Enhancement of Plant Disease Resistance Using CRISPR/Cas9 Technology. *Front Plant Sci*, 9: 1245. doi: 10.3389/fpls.2018.01245.

Bristow, P. R., McNicol, R. J. & Williamson, B. (1986). Infection of strawberry flowers by Botrytis cinerea and its relevance to grey mould development. *Annals of Applied Biology*, 109 (3): 545-554. doi: 10.1111/j.1744-7348.1986.tb03211.x.

Brutus, A., Sicilia, F., Macone, A., Cervone, F. & De Lorenzo, G. (2010). A domain swap approach reveals a role of the plant wall-associated kinase 1 (WAK1) as a receptor of

oligogalacturonides. *Proc Natl Acad Sci U S A*, 107 (20): 9452-7. doi: 10.1073/pnas.1000675107.
Chen, K., Song, M., Guo, Y., Liu, L., Xue, H., Dai, H. & Zhang, Z. (2019). MdMYB46 could enhance salt and osmotic stress tolerance in apple by directly activating stress-responsive signals. *Plant Biotechnol J*, 17 (12): 2341-2355. doi: 10.1111/pbi.13151.
Coego, A., Ramirez, V., Ellul, P., Mayda, E. & Vera, P. (2005). The H2O2-regulated Ep5C gene encodes a peroxidase required for bacterial speck susceptibility in tomato. *Plant J*, 42 (2): 283-93. doi: 10.1111/j.1365-313X.2005.02372.x.
Conrath, U., Pieterse, C. M. J. & Mauch-Mani, B. (2002). Priming in plant–pathogen interactions. *Trends in Plant Science*, 7 (5): 210-216. doi: 10.1016/s1360-1385(02)02244-6.
Conrath, U. (2009). Chapter 9 Priming of Induced Plant Defense Responses. In Advances in Botanical Research, pp. 361-395.
Cosio, C. & Dunand, C. (2010). Transcriptome analysis of various flower and silique development stages indicates a set of class III peroxidase genes potentially involved in pod shattering in Arabidopsis thaliana. *BMC Genomics*, 11: 528. doi: 10.1186/1471-2164-11-528.
Darras, A. I., Joyce, D. C., Terry, L. A. & Vloutoglou, I. (2006). Postharvest infection ofFreesia hybridaflowers byBotrytis cinerea. *Australasian Plant Pathology*, 35 (1). doi: 10.1071/ap05103.
de Jesus-Pires, C., Ferreira-Neto, J. R. C., Pacifico Bezerra-Neto, J., Kido, E. A., de Oliveira Silva, R. L., Pandolfi, V., Wanderley-Nogueira, A. C., Binneck, E., da Costa, A. F., Pio-Ribeiro, G., et al. (2020). Plant Thaumatin-like Proteins: Function, Evolution and Biotechnological Applications. *Curr Protein Pept Sci*, 21 (1): 36-51. doi: 10.2174/1389203720666190318164905.
De Lorenzo, G., Brutus, A., Savatin, D. V., Sicilia, F. & Cervone, F. (2011). Engineering plant resistance by constructing chimeric receptors that recognize damage-associated molecular patterns (DAMPs). *FEBS Lett*, 585 (11): 1521-8. doi: 10.1016/j.febslet.2011.04.043.

De Neergaard, E. (1997). *Methods in Botanical Histopathology*: Copenhagen, Denmark : Danish Government Institute of Seed Pathology for Developing Countries.
Degani, O. & Cernica, G. (2014). Diagnosis and Control of <i>Harpophora maydis</i>, the Cause of Late Wilt in Maize. *Advances in Microbiology*, 04 (02): 94-105. doi: 10.4236/aim.2014.42014.
Donati, I., Cellini, A., Buriani, G., Mauri, S., Kay, C., Tacconi, G. & Spinelli, F. (2018). Pathways of flower infection and pollen-mediated dispersion of Pseudomonas syringae pv. actinidiae, the causal agent of kiwifruit bacterial canker. *Hortic Res*, 5: 56. doi: 10.1038/s41438-018-0058-6.
Edger, P. P., Poorten, T. J., VanBuren, R., Hardigan, M. A., Colle, M., McKain, M. R., Smith, R. D., Teresi, S. J., Nelson, A. D. L., Wai, C. M., et al. (2019). Origin and evolution of the octoploid strawberry genome. *Nat Genet*, 51 (3): 541-547. doi: 10.1038/s41588-019-0356-4.
Eichmann, R., Bischof, M., Weis, C., Shaw, J., Lacomme, C., Schweizer, P., Duchkov, D., Hensel, G., Kumlehn, J. & Huckelhoven, R. (2010). BAX INHIBITOR-1 is required for full susceptibility of barley to powdery mildew. *Mol Plant Microbe Interact*, 23 (9): 1217-27. doi: 10.1094/MPMI-23-9-1217.
Elisabeth Lof, M., de Vallavieille-Pope, C. & van der Werf, W. (2017). Achieving Durable Resistance Against Plant Diseases: Scenario Analyses with a National-Scale Spatially Explicit Model for a Wind-Dispersed Plant Pathogen. *Phytopathology*, 107 (5): 580-589. doi: 10.1094/PHYTO-05-16-0207-R.
Elliott, A. D. (2020). Confocal Microscopy: Principles and Modern Practices. *Curr Protoc Cytom*, 92 (1): e68. doi: 10.1002/cpcy.68.
Evert, R. F. & Eichhorn, S. E. (2013). *Raven Biology of Plants*. 8 ed.: Peter Marshall.
FAOSTAT. (2020). Available at: http://www.fao.org/faostat/en/#data/QV (accessed: 25.12).
Ferrari, S., Plotnikova, J. M., De Lorenzo, G. & Ausubel, F. M. (2003). Arabidopsis local resistance to Botrytis cinerea involves salicylic acid and camalexin and requires EDS4 and PAD2, but not SID2, EDS5 or PAD4. *Plant J*, 35 (2): 193-205. doi: 10.1046/j.1365-313x.2003.01794.x.

Ferrari, S., Galletti, R., Denoux, C., De Lorenzo, G., Ausubel, F. M. & Dewdney, J. (2007). Resistance to Botrytis cinerea induced in Arabidopsis by elicitors is independent of salicylic acid, ethylene, or jasmonate signaling but requires PHYTOALEXIN DEFICIENT3. *Plant Physiol*, 144 (1): 367-79. doi: 10.1104/pp.107.095596.

Fister, A. S., Landherr, L., Maximova, S. N. & Guiltinan, M. J. (2018). Transient Expression of CRISPR/Cas9 Machinery Targeting TcNPR3 Enhances Defense Response in Theobroma cacao. *Front Plant Sci*, 9: 268. doi: 10.3389/fpls.2018.00268.

Garrido, C., Carbú, M., Fernández-Acero, F. J., González-Rodrígo, V. E. & Cantoral, J. M. (2011). New Insights in the Study of Strawberry Fungal Pathogens. *G3-Genes Genomes Genetics*, 5 (Special Issue 1): 24-39.

Gomez, M. A., Lin, Z. D., Moll, T., Chauhan, R. D., Hayden, L., Renninger, K., Beyene, G., Taylor, N. J., Carrington, J. C., Staskawicz, B. J., et al. (2019). Simultaneous CRISPR/Cas9-mediated editing of cassava eIF4E isoforms nCBP-1 and nCBP-2 reduces cassava brown streak disease symptom severity and incidence. *Plant Biotechnol J*, 17 (2): 421-434. doi: 10.1111/pbi.12987.

Gooding. (1976). Gooding, H.J. (1976) Resistance to mechanical injury and assessment

of shelf life in fruits of strawberry (Fragaria ananassa). Hort. Res.

16: 71–82.

Guo, H., Wang, Y., Wang, L., Hu, P., Wang, Y., Jia, Y., Zhang, C., Zhang, Y., Zhang, Y., Wang, C., et al. (2017). Expression of the MYB transcription factor gene BplMYB46 affects abiotic stress tolerance and secondary cell wall deposition in Betula platyphylla. *Plant Biotechnol J*, 15 (1): 107-121. doi: 10.1111/pbi.12595.

Halliday, K. J., Hudson, M., Ni, M., Qin, M. & Quail, P. H. (1999). poc1: an Arabidopsis mutant perturbed in phytochrome signaling because of a T DNA insertion in the promoter of PIF3, a gene encoding a phytochrome-interacting bHLH protein. *Proc Natl Acad Sci U S A*, 96 (10): 5832-7. doi: 10.1073/pnas.96.10.5832.

Han, G. Z. (2019). Origin and evolution of the plant immune system. *New Phytol*, 222 (1): 70-83. doi: 10.1111/nph.15596.

Huang, R., Li, G. Q., Zhang, J., Yang, L., Che, H. J., Jiang, D. H. & Huang, H. C. (2011). Control of postharvest Botrytis fruit rot of strawberry by volatile organic compounds of Candida intermedia. *Phytopathology*, 101 (7): 859-69. doi: 10.1094/PHYTO-09-10-0255.

Hückelhoven, R., Eichmann, R., Weis, C., Hoefle, C. & Proels, R. K. (2013). Genetic loss of susceptibility: a costly route to disease resistance? *Plant Pathology*, 62: 56-62. doi: 10.1111/ppa.12103.

Jacobo-Velazquez, D. A., Gonzalez-Aguero, M. & Cisneros-Zevallos, L. (2015). Cross-talk between signaling pathways: the link between plant secondary metabolite production and wounding stress response. *Sci Rep*, 5: 8608. doi: 10.1038/srep08608.

Jones, J. D. & Dangl, J. L. (2006). The plant immune system. *Nature*, 444 (7117): 323-9. doi: 10.1038/nature05286.

Kato-Nitta, N., Maeda, T., Inagaki, Y. & Tachikawa, M. (2019). Expert and public perceptions of gene-edited crops: attitude changes in relation to scientific knowledge. *Palgrave Communications*, 5 (1). doi: 10.1057/s41599-019-0328-4.

Keller, H., Boyer, L. & Abad, P. (2016). Disease susceptibility in the Zig-Zag model of host-microbe interactions: only a consequence of immune suppression? *Mol Plant Pathol*, 17 (4): 475-9. doi: 10.1111/mpp.12371.

Kim, W. C., Ko, J. H., Kim, J. Y., Kim, J., Bae, H. J. & Han, K. H. (2013). MYB46 directly regulates the gene expression of secondary wall-associated cellulose synthases in Arabidopsis. *Plant J*, 73 (1): 26-36. doi: 10.1111/j.1365-313x.2012.05124.x.

Kusch, S. & Panstruga, R. (2017). mlo-Based Resistance: An Apparently Universal "Weapon" to Defeat Powdery Mildew Disease. *Mol Plant Microbe Interact*, 30 (3): 179-189. doi: 10.1094/MPMI-12-16-0255-CR.

Lee, M. H., Jeon, H. S., Kim, S. H., Chung, J. H., Roppolo, D., Lee, H. J., Cho, H. J., Tobimatsu, Y., Ralph, J. & Park, O. K. (2019). Lignin-based barrier restricts pathogens to the infection site and confers resistance in plants. *EMBO J*, 38 (23): e101948. doi: 10.15252/embj.2019101948.

Li, L., Shi, Z. Y., Li, L., Shen, G. Z., Wang, X. Q., An, L. S. & Zhang, J. L. (2010). Overexpression of ACL1 (abaxially curled leaf 1) increased Bulliform cells and induced Abaxial curling of leaf blades in rice. *Mol Plant*, 3 (5): 807-17. doi: 10.1093/mp/ssq022.

Liu, G., Kennedy, R., Greenshields, D. L., Peng, G., Forseille, L., Selvaraj, G. & Wei, Y. (2007). Detached and attached Arabidopsis leaf assays reveal distinctive defense responses against hemibiotrophic Colletotrichum spp. *Mol Plant Microbe Interact*, 20 (10): 1308-19. doi: 10.1094/MPMI-20-10-1308.

Maghari, B. M. & Ardekani, A. M. (2011). Genetically modified foods and social concerns. *Avicenna J Med Biotechnol*, 3 (3): 109-17.

McCarthy, R. L., Zhong, R. & Ye, Z. H. (2009). MYB83 is a direct target of SND1 and acts redundantly with MYB46 in the regulation of secondary cell wall biosynthesis in Arabidopsis. *Plant Cell Physiol*, 50 (11): 1950-64. doi: 10.1093/pcp/pcp139.

Meng, L., Höfte, M. & Van Labeke, M.-C. (2019). Leaf age and light quality influence the basal resistance against Botrytis cinerea in strawberry leaves. *Environmental and Experimental Botany*, 157: 35-45. doi: 10.1016/j.envexpbot.2018.09.025.

Miedes, E., Vanholme, R., Boerjan, W. & Molina, A. (2014). The role of the secondary cell wall in plant resistance to pathogens. *Front Plant Sci*, 5: 358. doi: 10.3389/fpls.2014.00358.

Możdżeń, K., Bojarski, B., Rut, G., Migdałek, G., Repka, P. & Rzepka, A. (2015). Effect of drought stress induced by mannitol on physiological parameters of maize (Zea mays L.) seedlings and plants. *Journal of Microbiology, Biotechnology and Food Sciences*, 04 (Special issue 2): 86-91. doi: 10.15414/jmbfs.2015.4.special2.86-91.

Nellist, C. (2018). Disease resistance in polyploid strawberry. In Hytönen, T., Graham, J. & Harrison, R. (eds) Compendium of Plant Genomes, *The Genomes of Rosaceous Berries and Their Wild Relatives*, pp. 79-94: Springer International Publishing AG.

Park, D., Park, S. H., Ban, Y. W., Kim, Y. S., Park, K. C., Kim, N. S., Kim, J. K. & Choi, I. Y. (2017). A bioinformatics approach for identifying transgene insertion sites using whole genome sequencing data. *BMC Biotechnol*, 17 (1): 67. doi: 10.1186/s12896-017-0386-x.

Petrasch, S., Knapp, S. J., van Kan, J. A. L. & Blanco-Ulate, B. (2019). Grey mould of strawberry, a devastating disease caused by the ubiquitous necrotrophic fungal pathogen Botrytis cinerea. *Mol Plant Pathol*, 20 (6): 877-892. doi: 10.1111/mpp.12794.

Pfaffl, M. W. (2001). A new mathematical model for relative quantification in real-time RT-PCR. *Nucleic Acids Res*, 29 (9): e45. doi: 10.1093/nar/29.9.e45.

Quilliam, R. S., Swarbrick, P. J., Scholes, J. D. & Rolfe, S. A. (2006). Imaging photosynthesis in wounded leaves of Arabidopsis thaliana. *J Exp Bot*, 57 (1): 55-69. doi: 10.1093/jxb/erj039.

Rahman, M. H., Hjeljord, L. G., Aam, B. B., Sørlie, M. & Tronsmo, A. (2014). Antifungal effect of chito-oligosaccharides with different degrees of polymerization. *European Journal of Plant Pathology*, 141 (1): 147-158. doi: 10.1007/s10658-014-0533-3.

Ramirez, V., Agorio, A., Coego, A., Garcia-Andrade, J., Hernandez, M. J., Balaguer, B., Ouwerkerk, P. B., Zarra, I. & Vera, P. (2011a). MYB46 modulates disease susceptibility to Botrytis cinerea in Arabidopsis. *Plant Physiol*, 155 (4): 1920-35. doi: 10.1104/pp.110.171843.

Ramirez, V., Garcia-Andrade, J. & Vera, P. (2011b). Enhanced disease resistance to Botrytis cinerea in myb46 Arabidopsis plants is associated to an early down-regulation of CesA genes. *Plant Signal Behav*, 6 (6): 911-3. doi: 10.4161/psb.6.6.15354.

Redman, M., King, A., Watson, C. & King, D. (2016). What is CRISPR/Cas9? *Arch Dis Child Educ Pract Ed*, 101 (4): 213-5. doi: 10.1136/archdischild-2016-310459.

Ruan, J., Zhou, Y., Zhou, M., Yan, J., Khurshid, M., Weng, W., Cheng, J. & Zhang, K. (2019). Jasmonic Acid Signaling Pathway in Plants. *Int J Mol Sci*, 20 (10). doi: 10.3390/ijms20102479.

Shulaev, V., Sargent, D. J., Crowhurst, R. N., Mockler, T. C., Folkerts, O., Delcher, A. L., Jaiswal, P., Mockaitis, K., Liston, A., Mane, S. P., et al. (2011). The genome of woodland strawberry (Fragaria vesca). *Nat Genet*, 43 (2): 109-16. doi: 10.1038/ng.740.

Smith, R. A., Schuetz, M., Roach, M., Mansfield, S. D., Ellis, B. & Samuels, L. (2013). Neighboring parenchyma cells contribute to Arabidopsis xylem lignification, while lignification of

interfascicular fibers is cell autonomous. *Plant Cell*, 25 (10): 3988-99. doi: 10.1105/tpc.113.117176.
Song, G., Jia, M., Chen, K., Kong, X., Khattak, B., Xie, C., Li, A. & Mao, L. (2016). CRISPR/Cas9: A powerful tool for crop genome editing. *The Crop Journal*, 4 (2): 75-82. doi: 10.1016/j.cj.2015.12.002.
SSB. (2018). *Vi spiser mer utenlandske enn norske jordbær*. Available at: https://www.ssb.no/jord-skog-jakt-og-fiskeri/artikler-og-publikasjoner/vi-spiser-mer-utenlandske-enn-norske-jordbaer.
SSB. (2020). *Hagebruksavlingar: Tabell*. Available at: https://www.ssb.no/statbank/table/10508/ (accessed: 20.12).
Tian, X., Zhang, L., Feng, S., Zhao, Z., Wang, X. & Gao, H. (2019). Transcriptome Analysis of Apple Leaves in Response to Powdery Mildew (Podosphaera leucotricha) Infection. *Int J Mol Sci*, 20 (9). doi: 10.3390/ijms20092326.
Uknes, S., Mauch-Mani, B., Moyer, M., Potter, S., Williams, S., Dincher, S., Chandler, D., Slusarenko, A., Ward, E. & Ryals, J. (1992). Acquired resistance in Arabidopsis. *Plant Cell*, 4 (6): 645-56. doi: 10.1105/tpc.4.6.645.
UN. (2019a). *Sustainable Development Goals, 2. Zero Hunger*. Available at: https://www.un.org/sustainabledevelopment/hunger/ (accessed: 05.03).
UN. (2019b). *World Population Prospects 2019*. Available at: https://population.un.org/wpp/Graphs/DemographicProfiles/Line/900 (accessed: 01.02).
Uniprot. (2000). *UniProtKB - Q9M8Z8 (PLY8_ARATH)*. Available at: https://www.uniprot.org/uniprot/Q9M8Z8 (accessed: 27.06).
van Schie, C. C. & Takken, F. L. (2014). Susceptibility genes 101: how to be a good host. *Annu Rev Phytopathol*, 52: 551-81. doi: 10.1146/annurev-phyto-102313-045854.
Veljović Jovanović, S., Kukavica, B., Vidović, M., Morina, F. & Menckhoff, L. (2018). Class III Peroxidases: Functions, Localization and Redox Regulation of Isoenzymes. In Gupta, D. K., Palma, J. M. & Corpas, F. J. (eds) *Antioxidants and Antioxidant Enzymes in Higher Plants*, pp. 269-300. Cham: Springer International Publishing.

Wang, L. F., Li, T. T., Zhang, Y., Guo, J. X., Lu, K. K. & Liu, W. C. (2021). CAND2/PMTR1 Is Required for Melatonin-Conferred Osmotic Stress Tolerance in Arabidopsis. *Int J Mol Sci*, 22 (8). doi: 10.3390/ijms22084014.

Watkinson, S., Boddy, L. & Money, N. P. (2016). *The Fungi*. 3 ed.: Sara Tenney.

Williamson, B., Tudzynski, B., Tudzynski, P. & van Kan, J. A. (2007). Botrytis cinerea: the cause of grey mould disease. *Mol Plant Pathol*, 8 (5): 561-80. doi: 10.1111/j.1364-3703.2007.00417.x.

Wilson, F. M., Harrison, K., Armitage, A. D., Simkin, A. J. & Harrison, R. J. (2019). CRISPR/Cas9-mediated mutagenesis of phytoene desaturase in diploid and octoploid strawberry. *Plant Methods*, 15: 45. doi: 10.1186/s13007-019-0428-6.

Zhong, R., Richardson, E. A. & Ye, Z. H. (2007). The MYB46 transcription factor is a direct target of SND1 and regulates secondary wall biosynthesis in Arabidopsis. *Plant Cell*, 19 (9): 2776-92. doi: 10.1105/tpc.107.053678.

Zhong, R., Lee, C., McCarthy, R. L., Reeves, C. K., Jones, E. G. & Ye, Z. H. (2011). Transcriptional activation of secondary wall biosynthesis by rice and maize NAC and MYB transcription factors. *Plant Cell Physiol*, 52 (10): 1856-71. doi: 10.1093/pcp/pcr123.

Zhou, W., Karcher, D. & Bock, R. (2014). Identification of enzymes for adenosine-to-inosine editing and discovery of cytidine-to-uridine editing in nucleus-encoded transfer RNAs of Arabidopsis. *Plant Physiol*, 166 (4): 1985-97. doi: 10.1104/pp.114.250498.

Norges miljø- og biovitenskapelige universitet
Noregs miljø- og biovitskapelege universitet
Norwegian University of Life Sciences

Postboks 5003
NO-1432 Ås
Norway